

NON-PEER-REVIEWED PREPRINT

Submitted to EarthArXiv

Identification and Verification of Worst-Case Radiological Transport Scenarios for Ireland: A Simulation-Based Approach to Nuclear Emergency Preparedness (2011–2024)

Marc Sturrock^{1,2}, *marcsturrock@rcsi.ie*

<https://orcid.org/0000-0002-7435-5256>

Robert Ryan², *R.Ryan@epa.ie*

Kevin Kelleher², *K.Kelleher@epa.ie*

¹Department of Physiology and Medical Physics, Royal College of Surgeons in Ireland, Dublin, Ireland

²Office of Radiation Protection and Environmental Monitoring, Environmental Protection Agency, McCumiskey House, Richview, Clonskeagh Road, Dublin 14, Ireland

This manuscript is a non-peer-reviewed preprint submitted to EarthArXiv.
It has not yet been submitted to a journal for peer review.

January 2026

Identification and Verification of Worst-Case Radiological Transport Scenarios for Ireland: A Simulation-Based Approach to Nuclear Emergency Preparedness (2011-2024)

Marc Sturrock^{1,2}, Robert Ryan², Kevin Kelleher²

¹*Department of Physiology and Medical Physics, Royal College of Surgeons in Ireland, Dublin, Ireland*

²*Office of Radiation Protection and Environmental Monitoring, Environmental Protection Agency, McCumiskey House, Richview, Clonskeagh Road, Dublin 14, Ireland*

January 19, 2026

This study presents a comprehensive simulation-based assessment of potential transboundary radiological transport to Ireland from six nuclear facilities in the United Kingdom and France, utilising weather data over a fourteen-year period (2011–2024). Systematic screening of 2.2 million HYSPLIT atmospheric dispersion simulations identified eighteen worst-case scenarios representing conditions of maximum ground deposition, maximum air concentration, and minimum warning time for protective action implementation. Independent verification using FLEXPART and HYSPLIT demonstrated expected inter-model variability (factor of 1–10), with both Lagrangian models providing consistent risk assessment brackets. Heysham, despite its complex 19-isotope AGR source term, produced negligible radiological doses to Ireland (< 0.01 mSv)—more than four orders of magnitude below intervention thresholds. More distant continental facilities (Flamanville, Paluel, Sizewell B) showed low but measurable doses (0.1–4.6 mSv depending on scenario and model), remaining well below the 50 mSv sheltering threshold. Hinkley Point C (under construction) showed elevated but sub-threshold doses (0.3–8.5 mSv depending on model). However, the cancelled Wylfa Newydd gigawatt-scale project (the site is now proposed for small modular reactors), owing to its extreme proximity to Ireland, exhibited concerning dose predictions: FLEXPART calculated 20.7 mSv under maximum deposition conditions (May 2024 scenario), approaching the 50 mSv sheltering threshold, whilst HYSPLIT predicted 4.5 mSv. This inter-model variability (factor of ~5) highlights genuine uncertainty for near-source impacts but converges on a critical finding: were a gigawatt-scale reactor constructed at the Wylfa site, severe accidents during specific meteorological patterns could require protective actions in Ireland. Machine learning models (XGBoost) achieved validation accuracies of 85–93% for rapid impact prediction, whilst global sensitivity analysis revealed that meteorological conditions, rather than release parameters, dominate consequence severity. These findings provide quantitative assurance that existing nuclear infrastructure poses low transboundary risk to Ireland well below intervention thresholds, whilst demonstrating that facility proximity constitutes the dominant factor determining potential radiological impact.

1 Introduction

The Environmental Protection Agency (EPA) plays a pivotal role as a national principal support agency in Ireland, tasked with responding to nuclear or radiological emergencies that could affect the nation. A critical component of this responsibility is the provision of robust technical support and evidence-based advice to the National Emergency Co-ordination Group. This support is substantially reliant on the application of medium and long-range atmospheric dispersion models. These models are instrumental in predicting the trajectory, extent, and potential consequences of radioactive material released into the atmosphere, typically originating from nuclear accidents at facilities abroad. Key model outputs, such as predicted radioactive deposition on terrestrial surfaces, ambient air concentrations, and precise plume arrival times, are fundamental for estimating the potential radiological implications for Ireland. Such estimations are vital for informing timely and effective decisions regarding protective actions, which may include recommendations for public sheltering or the safeguarding of agricultural resources like livestock [19]. This study focuses principally on protective actions in the early phase of a nuclear emergency; protective actions related to food controls arising from the uptake of radionuclides into the food chain are beyond the scope of the present analysis.

Previous work, such as the 2013 report by the Radiological Protection Institute of Ireland (RPII) [27], assessed the potential radiological impacts on Ireland from proposed new nuclear power plants in the UK. That study considered both routine discharges and a range of postulated accident scenarios, utilising specific weather patterns designed to maximise radioactive transfer to Ireland. For severe accidents, the RPII (2013) report highlighted that weather conditions were a dominant factor, with most scenarios not resulting in direct atmospheric transport over Ireland, but noted that under specific adverse conditions, protective actions including sheltering and food controls would be necessary [27]. Subsequent assessments, including the 2016 EPA evaluation of postulated accidents at the Sellafield nuclear fuel reprocessing plant, similarly employed atmospheric dispersion modelling to identify worst-case scenarios and concluded that doses would remain below international intervention thresholds [10]. More recently, Joy (2020) conducted comprehensive modelling of accidental radioactive releases for Ireland, comparing HYSPLIT and FLEXPART model performance with ECMWF meteorological data and emphasising the value of ensemble modelling approaches for emergency preparedness [22]. Whilst these previous studies provided valuable insights, they were typically limited to single-site assessments or restricted temporal sampling of meteorological conditions, motivating the present comprehensive, multi-site, fourteen-year systematic analysis.

The selection of appropriate atmospheric transport and dispersion models is critical for emergency preparedness. Lagrangian particle dispersion models have emerged as the preferred methodology for simulating long-range transport from nuclear facilities, offering fundamental advantages over Eulerian grid-based approaches. The HYSPLIT (Hybrid Single-Particle Lagrangian Integrated Trajectory) model, developed by NOAA's Air Resources Laboratory, has been extensively validated for long-range atmospheric transport and serves as a cornerstone of operational emergency response systems worldwide [8, 40]. HYSPLIT employs a hybrid computational approach, utilising a Lagrangian reference frame for calculating particle advection and diffusion whilst computing concentrations on a fixed Eulerian grid. The model has demonstrated strong performance in validation studies against monitoring data from the Fukushima Daiichi Nuclear Power Plant accident [6, 15], confirming its capability to accurately simulate transboundary transport of radioactive material.

The FLEXPART (FLEXible PARTicle dispersion model) provides an independent Lagrangian framework specifically designed for simulating long-range dispersion of pollutants from point sources [41]. Originally validated against large-scale tracer experiments [42], FLEXPART has undergone continuous development with recent versions incorporating improved parameterisations for turbulent mixing and wet deposition [2, 32]. The fundamental advantage of Lagrangian models over Eulerian approaches lies in their freedom from numerical diffusion: Lagrangian particle trajectories retain spatial resolution independent of the computational grid, preserving plume structure during long-range transport where Eulerian models would artificially dilute the plume through repeated grid-cell averaging.

Model intercomparison studies have consistently demonstrated that atmospheric dispersion predictions contain inherent uncertainties arising from meteorological inputs, physical parameterisations, and numerical implementations [12, 48]. The ENSEMBLE and SEED intercomparison exercises, comparing multiple models for hypothetical nuclear accidents, revealed that multi-model ensemble approaches generally outperform individual deterministic simulations, particularly for complex meteorological regimes [12]. More recent

intercomparisons, including the multi-model ^{137}Cs dispersion study from the Fukushima Daiichi accident using identical input data, demonstrated that models perform better near the source than at regional scales, with inter-model spread indicating structural model uncertainties [35]. Recent studies have also explored meteorological ensemble forecasting to quantify dispersion uncertainty, demonstrating that whilst ensemble approaches capture meteorological variability, they require extensive computational resources [25]. This body of evidence has significant implications for emergency response: verifying worst-case scenarios using independent models with identical meteorological forcing provides confidence that identified transport patterns represent genuine physical phenomena rather than model-specific artefacts or meteorological input differences.

Radiological consequence assessment requires coupling atmospheric transport predictions with appropriate source terms and dose conversion methodologies. Severe accident source terms are typically derived from Level 2 probabilistic risk assessment, characterising the timing, duration, and isotopic composition of atmospheric releases following core damage and containment failure [38]. Post-Fukushima source term reconstructions using inverse modelling and atmospheric observations have demonstrated the importance of realistic accident progression physics, including containment retention and aerosol depletion mechanisms, which substantially reduce environmental releases relative to total core inventory [4, 36]. The International Commission on Radiological Protection provides authoritative dose coefficients for converting atmospheric concentrations and ground deposition into effective dose through multiple pathways including inhalation, cloudshine, and groundshine [9, 17, 18, 31]. Integration of these standardised methodologies ensures that predicted doses can be directly compared against international intervention thresholds and emergency reference levels.

This current study aims to significantly enhance and broaden the EPA's preparedness by systematically reviewing and updating the inputs and methodologies for these atmospheric dispersion models, and by conducting a comprehensive assessment of potential radiological transport pathways. The scope of this research is informed by several evolving factors: the ongoing development of new nuclear facilities across Europe, the operational extensions of many existing plants, and the dynamic nature of the international nuclear safety landscape, which includes considering the potential implications arising from geopolitical events, such as the conflict in Ukraine, on nuclear facility safety and security.

This study employs a systematic, multi-method approach to identify and verify worst-case radiological transport scenarios that could impact Ireland. The research integrates large-scale atmospheric dispersion modelling, independent model verification, machine learning for impact prediction, and global sensitivity analysis to provide a comprehensive, quantitative basis for emergency preparedness planning.

The primary objective is the systematic identification of worst-case meteorological scenarios through large-ensemble HYSPLIT (Hybrid Single-Particle Lagrangian Integrated Trajectory) screening over a fourteen-year period (2011–2024), substantially longer than previous Irish assessments. This extensive temporal coverage encompasses six nuclear facilities in proximity to Ireland, with parametric variations in release height (20–100 m) and duration (6–48 h) to capture the full spectrum of potential accident conditions. Initial simulations employed unit releases to isolate atmospheric transport characteristics, enabling the identification of high-consequence scenarios based on total deposition (mass/m²), average air concentration (mass/m³), and plume arrival times over Irish territory.

An important component of this study is the independent verification of all identified scenarios using the FLEXPART Lagrangian particle dispersion model. This dual-model approach provides confidence that identified transport patterns and radiological consequences represent genuine emergency planning concerns rather than model-specific artefacts. For each worst-case scenario, realistic source terms representing severe accident conditions (core melt with late containment failure) were applied, scaled to each NPP's thermal power, to calculate potential dose distributions across Ireland. The agreement between two independent dispersion models strengthens confidence in the robustness of the identified scenarios for protective action planning.

Beyond scenario identification and verification, the research develops predictive capability through machine learning (XGBoost) with cross-validated champion models to enable rapid impact assessment during emergencies. Global sensitivity analysis using Sobol indices quantifies which physical and release parameters most strongly influence radiological consequences, providing critical insights for monitoring priorities and model refinement. Crucially, both the machine learning and sensitivity analysis methodologies leverage the extensive simulation ensemble (2.2 million scenarios) originally generated for worst-case identification, maximising the scientific and operational value extracted from this substantial computational investment. Collectively, these methods establish a contemporary, evidence-based foundation for Ireland's nuclear emer-

gency response strategies.

The structure of this paper is organised as follows. Section 2 describes the pipelines for identifying worst-case scenario NPP incidents for Ireland, the atmospheric dispersion modelling frameworks employed (HYSPPLIT and FLEXPART), model verification approach, source term definitions, radiological dose assessment methodology, machine learning model development, and sensitivity analysis techniques. Section 3 presents the identified worst-case scenarios, independent FLEXPART verification, radiological dose assessments, machine learning performance, and sensitivity analysis findings. Section 4 interprets the results in the context of emergency preparedness, discusses model uncertainty and robustness, and identifies critical parameters for monitoring and decision-making. Section 5 summarises key findings and recommendations for Ireland’s ongoing preparedness enhancement.

2 Methodology

2.1 Nuclear Facilities Considered

This study assessed six nuclear facilities in the United Kingdom and France that are proximal to Ireland and represent potential sources of transboundary radiological impact. The facilities span a range of reactor technologies, operational statuses, and distances from Ireland (measured from Dublin, 53.35°N, 6.26°W), providing a comprehensive assessment of the nuclear landscape relevant to Irish emergency preparedness.

Wylfa (53.42°N, 4.48°W, ~130 km) on the Isle of Anglesey, Wales, is the closest potential nuclear site to Ireland. The original Magnox station ceased operations in 2015. The proposed Wylfa Newydd project (two 1.35 GW_e EPR units) was cancelled in 2020; however, the site has subsequently been identified for potential small modular reactor (SMR) development by Rolls-Royce (470 MW_e PWR design). This study models the originally proposed gigawatt-scale EPR configuration, representing an upper-bound worst-case scenario; actual SMR consequences would be substantially lower due to reduced thermal power and core inventory.

Heysham (54.03°N, 2.91°W, ~250 km) in Lancashire comprises two operational Advanced Gas-cooled Reactor (AGR) stations: Heysham 1 (2 × 580 MW_e, operational since 1983) and Heysham 2 (2 × 615 MW_e, operational since 1988). AGR source terms differ substantially from PWR releases, incorporating a broader isotope spectrum including actinides (plutonium, americium, curium) and additional fission products (strontium, ruthenium, cerium), necessitating a 19-isotope source term for this facility compared to 4 isotopes for PWR/EPR sites.

Hinkley Point C (51.21°N, 3.14°W, ~340 km) in Somerset is currently under construction, comprising two 1.63 GW_e EPR units. When operational (expected mid-2030s), it will be the UK's largest nuclear power station. The EPR design incorporates enhanced safety features including a core catcher and double containment.

Sizewell B (52.22°N, 1.62°E, ~480 km) in Suffolk is the UK's only operating PWR (1.2 GW_e, operational since 1995). A sister station (Sizewell C, 2 × EPR) has received development consent but construction has not yet commenced.

Flamanville (49.54°N, 1.88°W, ~550 km) in Normandy, France, hosts two operational PWR units (2 × 1.33 GW_e, operational since 1986–1987) and one EPR unit (1.65 GW_e) that achieved first criticality in 2024 after extended construction delays.

Paluel (49.86°N, 0.64°E, ~650 km), also in Normandy, is France's largest nuclear station with four PWR units (4 × 1.33 GW_e, operational since 1984–1986). Its position on the English Channel coast and substantial combined thermal power make it relevant for Irish emergency planning despite being the most distant facility considered.

2.2 Atmospheric Dispersion Modelling

The atmospheric transport and dispersion modelling framework employed two independent Lagrangian particle dispersion models: HYSPLIT (Hybrid Single-Particle Lagrangian Integrated Trajectory) and FLEXPART (FLEXible PARTicle dispersion model). This dual-model approach enables quantification of inter-model variability and provides verification that identified worst-case scenarios represent robust atmospheric transport patterns rather than model-specific artefacts.

HYSPLIT served as the primary screening tool for identifying worst-case scenarios across the fourteen-year study period (2011–2024). The model was configured with a hybrid computational scheme, employing Lagrangian particle trajectories for advection and diffusion calculations whilst computing concentrations on a fixed Eulerian output grid. Meteorological forcing utilised ERA5 reanalysis data from the European Centre for Medium-Range Weather Forecasts, accessed via HYSPLIT-compatible ARL-format files providing hourly meteorological fields at 0.25-degree horizontal resolution [16]. The selection of ERA5 over older reanalysis datasets (e.g., ERA-Interim) is critical for long-range transport studies: comparative analyses demonstrate that ERA5 provides superior representation of atmospheric boundary layer height (correlation 0.88 vs radiosondes) and vertical transport processes, with improved assimilation of satellite observations and better resolution of meso- to synoptic-scale meteorological features [14, 45]. Validation studies over European marine environments confirm ERA5's robust performance for offshore wind fields, which are particularly relevant for Irish Sea transboundary transport [5]. The model's vertical structure incorporated 25 output levels ranging from the surface to 3000 metres above ground level, with enhanced resolution in the atmospheric

boundary layer (0, 20, 30, 40, 50, 60, 80, 100, 150, 200, 250, 300, 400, 500, 600, 750, 1000, 1250, 1500, 1750, 2000, 2250, 2500, 2750, and 3000 m). This vertical distribution provides enhanced resolution near the surface where concentration gradients are steepest and human exposure is most relevant: seven levels within the breathing zone (0–100 m) enable precise calculation of inhalation doses, whilst the continued vertical spacing through the boundary layer and lower troposphere captures the evolution of boundary layer mixing, which dominates near-surface concentration patterns and determines ground-level deposition rates.

The HYSPLIT screening simulations employed unit releases (1 kg total mass) to isolate atmospheric transport characteristics from source term uncertainties. Each simulation released computational particles at rates of 500 particles per hour for release durations of 6 h (3000 particles total), 24 h (12,000 particles), or 48 h (24,000 particles). Simulations were executed for every day of the fourteen-year period at release hours 0, 3, 6, 9, 12, 15, 18, and 21 UTC, combined with three release heights (20, 50, 100 m above ground level), yielding 367,200 simulations per nuclear power plant. The computational domain extended from 10.47°W to 6.01°E longitude and from 51.45°N to 55.38°N latitude, encompassing Ireland, the UK, and portions of continental Europe with 0.25-degree horizontal resolution.

The large-scale simulation campaign (2.2 million scenarios across six nuclear power plants) was executed using a custom-built automation pipeline implemented in Julia, employing distributed parallel processing across 31 computational cores. The pipeline systematically generated HYSPLIT control files for each parameter combination (date, release hour, duration, height, and facility), executed simulations, processed output concentration fields and particle trajectory files, and automatically identified scenarios yielding atmospheric transport to Irish territory using point-in-polygon geometric algorithms applied to a high-resolution Republic of Ireland boundary definition (Northern Ireland was excluded from the analysis domain). A checkpointing system with persistent state management enabled resumable execution following interruptions, crucial for managing the multi-month computational campaign spanning fourteen years of meteorological conditions. This automated framework ensured systematic coverage of the complete parameter space whilst maintaining computational efficiency, result consistency, and traceability of the 367,200 simulations per facility.

Deposition processes were parameterised to represent typical aerosol behaviour characteristic of fission products released during severe accidents. Dry deposition employed a constant deposition velocity of 0.005 m s^{-1} , a value empirically validated from Chernobyl ^{137}Cs measurements representing the mean deposition rate over heterogeneous terrain and adopted as the standard parameter in HYSPLIT regional-scale simulations [28, 37]. This value falls at the conservative upper end of measured caesium aerosol deposition velocities ($1\text{--}5 \text{ mm s}^{-1}$) [43] and has demonstrated superior agreement with observed contamination patterns compared to complex resistance-based schemes for regional applications. Wet deposition utilised scavenging coefficients of 5.0×10^{-5} for both in-cloud and below-cloud removal processes, with precipitation fields derived directly from ERA5 data. Noble gases were treated as non-depositing tracers with negligible deposition parameters. Radioactive decay was not applied during the screening phase to preserve the unit-release framework; decay corrections were implemented subsequently during radiological dose assessment using isotope-specific half-lives.

FLEXPART version 10.4 provided independent verification of identified worst-case scenarios. The model employs a purely Lagrangian framework, computing particle trajectories using three-dimensional wind fields with stochastic perturbations representing turbulent diffusion. FLEXPART's convective parameterisation (LCONVECTION=1) explicitly represents sub-grid scale vertical transport in developing cumulus clouds, a process particularly relevant for daytime boundary layer evolution. The model utilised identical ERA5 meteorological forcing as HYSPLIT, ensuring that inter-model differences reflected physical parameterisations rather than meteorological inconsistencies.

For verification simulations, FLEXPART employed 5000 to 12,000 computational particles depending on release complexity, providing statistical robustness of concentration fields. The output grid matched HYSPLIT specifications exactly (identical horizontal extent, resolution, and vertical levels) to enable direct point-by-point comparison. Deposition parameterisations were harmonised with HYSPLIT settings: dry deposition velocity 0.005 m s^{-1} , wet scavenging coefficients 5.0×10^{-5} , and isotope-specific material densities ranging from 1879 kg m^{-3} (cesium) to $19,860 \text{ kg m}^{-3}$ (plutonium). Care was taken to account for unit system differences: FLEXPART expects densities in SI units (kg m^{-3}) whilst HYSPLIT requires CGS units (g cc^{-1}), necessitating division by 1000 for HYSPLIT input. Radioactive decay was implemented using isotope-specific half-lives during dose assessment calculations.

2.3 Element-Specific Deposition Parameters

Radionuclide transport and deposition were parameterised according to element-specific chemical properties, recognising that different elements exhibit distinct atmospheric behaviours due to variations in hygroscopicity, solubility, and particle formation characteristics. Table 1 presents the element-specific parameters employed for both HYSPLIT and FLEXPART simulations.

Table 1: Element-specific deposition parameters for radionuclide transport modelling

Element Category	Elements	Scavenging (1/s)	Dry Velocity (m/s)	CCN Efficiency	Chemical Basis
Noble Gases	Xe, Kr	0.0	0.0	0.0	Chemically inert
Soluble	Cs, I	1.0×10^{-4}	0.0015–0.002	0.9	Hygroscopic salts
Aerosols	Te, Sr	8.0×10^{-5}	0.0015	0.8	Soluble oxides
	Ru	5.0×10^{-5}	0.001	0.6	Lower solubility
Insoluble/Refractory	Pu, Am, Cm	2.0×10^{-5}	0.005	0.2	Insoluble ceramics
	Ce	3.0×10^{-5}	0.002	0.3	Refractory oxide

The physical rationale for these parameterisations reflects fundamental differences in atmospheric chemistry [23, 39]. Caesium and iodine form highly hygroscopic salts (CsOH , CsI , I_2) with strong affinity for water vapour, exhibiting high cloud condensation nuclei (CCN) efficiency and rapid wet scavenging. Actinides (Pu, Am, Cm) form refractory oxide ceramics with minimal water solubility, requiring higher dry deposition velocities but showing reduced wet removal. Noble gases remain chemically inert with zero deposition. Parameter values represent central estimates within the typical uncertainty range of factors of 2–5 for wet and dry deposition parameterisations [39]; sensitivity to meteorological and release parameters is explored in Section 2.8. Both FLEXPART and HYSPLIT employed identical element-specific parameters to ensure consistent physics between models, enabling valid inter-model comparison of predicted dose distributions.

2.4 Model Verification Approach

The model verification strategy addresses a fundamental challenge in emergency preparedness: atmospheric dispersion models contain inherent uncertainties arising from simplified physical parameterisations, finite spatial resolution, and meteorological input errors [12]. Reliance on a single model for identifying worst-case scenarios risks conflating genuine high-consequence transport patterns with model-specific numerical artefacts. The verification approach employed in this study ensures that all identified worst-case scenarios exhibit consensus between two independent Lagrangian models, thereby providing confidence that predicted transport patterns and radiological consequences represent robust emergency planning concerns.

Following completion of the HYSPLIT screening phase, the highest-consequence scenarios for each nuclear power plant (maximum total deposition, maximum average air concentration, minimum plume arrival time) were selected for detailed verification. These scenarios, identified using unit-release simulations, were re-run using both HYSPLIT and FLEXPART with realistic multi-isotope source terms representing severe accident conditions. The source terms incorporated reactor-specific radionuclide inventories scaled according to thermal power, with release fractions and isotopic compositions derived from Level 2 probabilistic safety assessment for late containment failure scenarios [1, 38].

The verification analysis quantified inter-model agreement through three complementary metrics. Spatial correlation coefficients evaluated the degree to which both models predicted similar geographical patterns of ground-level deposition and time-integrated air concentration across Ireland. Normalised root-mean-square differences quantified the magnitude of inter-model divergence relative to mean predicted values, with values below 0.5 indicating strong agreement and values exceeding 1.0 suggesting substantial model-dependent uncertainty. Peak concentration ratios compared the maximum predicted values from each model, identifying whether extreme values represented model consensus or outliers.

An important methodological distinction concerns deposition field representation. FLEXPART provides explicit wet and dry deposition output fields calculated through its integrated deposition schemes. HYSPLIT’s groundshine dose calculations employed in this study utilise near-surface (0 m) air concentration fields as a well-established proxy for deposited material, a standard approach in operational HYSPLIT dose

assessment [8]. This methodological difference is considered when interpreting inter-model differences in deposition-driven dose pathways, particularly for groundshine contributions where surface contamination fields drive external exposure estimates.

Concentration field comparisons were conducted at multiple vertical levels within the atmospheric boundary layer (0, 50, 100, 200, 500, 1000 m above ground level) to assess whether inter-model agreement varied with altitude. This vertical analysis addresses the potential for models to diverge in their representation of vertical mixing processes, particularly during convective conditions when boundary layer depth evolves rapidly. Time-series comparisons at fixed receptor locations quantified temporal consistency, verifying that both models predicted similar plume arrival times, concentration build-up rates, and exposure durations.

The radiological dose calculations provided the ultimate verification metric, integrating spatial concentration patterns, temporal evolution, and multi-isotope contributions through internationally standardised dose conversion factors. Agreement in predicted total effective dose distributions across Ireland constitutes the most policy-relevant verification measure, as emergency response decisions depend on dose magnitudes relative to intervention thresholds rather than concentration values per se. Verification simulations that demonstrated dose agreement within a factor of two between models were classified as robust worst-case scenarios suitable for emergency planning applications.

2.5 Worst-Case Scenario Identification

The systematic identification of worst-case scenarios proceeded through a multi-stage computational approach designed to isolate the atmospheric conditions and release parameters yielding maximum radiological consequences for Ireland. The methodology balanced computational efficiency—enabling analysis of 367,200 simulations per facility—with sufficient parametric coverage to capture the full range of plausible accident conditions.

The screening phase employed unit releases (1 kg total mass) to decouple atmospheric transport physics from source term uncertainties. This approach enabled direct comparison of atmospheric transport efficiency across different meteorological regimes without confounding effects from varying radionuclide inventories or isotopic compositions. Three output metrics characterised the severity of each simulated scenario: total deposition (mass per square metre integrated over Irish territory), average air concentration (mass per cubic metre averaged over Ireland for the simulation duration), and plume arrival time (hours from release until first detection of airborne material over Ireland).

Release parameters were varied systematically to span the range of severe accident conditions. Release heights of 20, 50, and 100 metres above ground level represented different degrees of initial plume buoyancy, with lower releases characteristic of filtered vented containment and higher releases representing unfiltered stack releases or thermal buoyancy from heat-driven releases. Release durations of 6, 24, and 48 hours captured both short-duration breach scenarios and protracted releases associated with gradual containment degradation. The combination of three release heights and three durations yielded nine release configurations, each executed at eight times of day (0, 3, 6, 9, 12, 15, 18, 21 UTC) to capture diurnal variations in atmospheric stability and wind patterns.

Temporal coverage extended from 1 January 2011 through 31 December 2024, providing fourteen years of historical and near-present meteorological conditions. This period substantially exceeds previous Irish assessments, which typically examined individual years or limited seasonal samples. The extended temporal coverage ensures that identified worst-case scenarios represent genuinely extreme atmospheric conditions rather than artefacts of limited sampling. The fourteen-year period encompasses multiple phases of the North Atlantic Oscillation, capturing both typical westerly flow regimes and anomalous easterly transport patterns that favour transport from continental Europe toward Ireland.

For each nuclear power plant, the complete set of simulations was ranked according to each output metric. The scenario yielding maximum total deposition was identified as the worst-case for long-term contamination and agricultural impacts. The scenario producing maximum average air concentration represented the worst-case for acute inhalation exposure. Scenarios with minimum plume arrival time identified conditions providing least warning time for protective action implementation. These three scenarios per nuclear power plant (18 scenarios total across six facilities) constituted the priority cases for detailed FLEXPART verification and radiological dose assessment.

2.6 Radiological Dose Assessment

Radiological dose assessment translates predicted atmospheric concentrations and ground deposition into effective dose, enabling direct comparison against international intervention thresholds and emergency reference levels. The methodology followed internationally standardised frameworks established by the International Commission on Radiological Protection [9, 17, 31], ensuring consistency with emergency planning guidance adopted by regulatory authorities in Ireland and neighbouring countries.

Severe accident source terms were developed for all six nuclear power plants through thermal power scaling from reference designs. Pressurised water reactor (PWR) and European Pressurised Reactor (EPR) source terms employed a four-isotope simplified inventory (tellurium-132, iodine-131, xenon-133, cesium-137) representing volatile fission products expected during late containment failure scenarios. The isotopic release fractions (approximately 5.4% of core iodine-131 inventory and 5.5% of cesium-137 inventory) represent the net environmental release after accounting for in-containment depletion processes, consistent with environmental release magnitudes for scenarios where containment failure occurs many hours after core melt initiation [38]. During this extended pre-release period, natural aerosol depletion processes (gravitational settling, diffusiophoresis, thermophoresis) remove 90–95% of condensable fission products from the containment atmosphere, substantially reducing the environmental release relative to core inventory.

Activities were scaled according to each reactor's thermal power rating using the relationship: $\text{Activity}_{\text{target}} = \text{Activity}_{\text{reference}} \times (\text{MW}_{\text{th,target}}/\text{MW}_{\text{th,reference}})$. The reference source term derived from French P'4 PWR design documentation (3817 MW_{th}), with Flamanville and Paluel employing unscaled reference values, Hinkley Point C and Wylfa scaled by a factor of 1.185 (4524 MW_{th} EPR design), and Sizewell B scaled by 0.911 (3479 MW_{th} Westinghouse PWR). The Heysham Advanced Gas-Cooled Reactor source term incorporated 19 radionuclides including actinides (plutonium-238/239/240/241, americium-241, curium-242/244), reflecting the fundamentally different core characteristics and accident phenomenology of graphite-moderated gas-cooled reactors: higher graphite dust generation, enhanced oxidation of metallic fuel cladding, and increased volatilisation and transport of low-volatility species including actinides compared to water-cooled designs.

Release rates (Becquerels per minute) were computed by dividing total isotope activity by release duration in minutes, ensuring uniform temporal distribution of emissions. This parameterisation required conversion between activity-based source terms (the standard specification in Level 2 probabilistic safety assessment) and mass-based model inputs (required by both HYSPLIT and FLEXPART). The conversion employed isotope-specific activities calculated from half-life and atomic mass: $\lambda_{\text{isotope}} = (\ln 2 \times N_A)/(t_{1/2} \times M)$, where N_A represents Avogadro's number, $t_{1/2}$ the half-life in seconds, and M the molar mass in kilograms per mole. Short-lived isotopes such as iodine-132 (half-life 2.3 hours) exhibit specific activities exceeding 10^{19} Bq kg⁻¹, whilst long-lived isotopes like cesium-137 (half-life 30.2 years) possess specific activities near 3×10^{15} Bq kg⁻¹.

Dose calculations integrated three exposure pathways following ICRP methodology. Inhalation dose was computed by time-integrating ground-level air concentrations (Becquerels per cubic metre) over the simulation duration, multiplying by a standard breathing rate (1.2 cubic metres per hour for light activity adults [17]), and applying isotope-specific committed effective dose coefficients (Sieverts per Becquerel inhaled). Cloudshine dose was calculated by integrating the three-dimensional concentration field (accounting for contributions from all altitudes) and applying external dose-rate coefficients for photon exposure from an infinite cloud geometry [31]. Groundshine dose utilised time-integrated ground deposition (Becquerels per square metre) multiplied by isotope-specific dose-rate coefficients for external exposure from contaminated ground surfaces, assuming a semi-infinite plane source geometry [31].

Total effective dose at each grid location represented the sum of all three pathways across all radionuclides. The dose calculations employed HYSPLIT's CON2REM utility with the -d1 flag for total dose output, implementing the coefficient database derived from ICRP publications. Dose distributions were computed across the full model domain at 0.25-degree resolution, with particular focus on maximum values over Irish territory and population-weighted averages accounting for settlement patterns. The resulting dose fields enable direct assessment against international and national intervention criteria: the IAEA generic criterion of 100 mSv projected dose over the first 7 days for urgent protective actions (sheltering and evacuation) [20], and Irish national intervention levels of 50 mSv for sheltering and 100 mSv for evacuation [11]. Iodine thyroid blocking (ITB) is recommended when projected thyroid equivalent doses from radioiodine inhalation exceed 50 mSv for children and 500 mSv for adults [11]; the predicted total effective doses in this study remain substantially below these thresholds for existing operational facilities, indicating that ITB would not be warranted for transboundary exposure from distant sites under worst-case conditions.

2.7 Machine Learning for Impact Prediction

The extensive dataset generated through fourteen years of HYSPLIT screening simulations (approximately 2.2 million simulations across six nuclear power plants) provided a unique opportunity to develop predictive models capable of rapid impact assessment during emergency conditions. Rather than treating the simulation ensemble solely as a worst-case identification tool, this approach maximises the value of the substantial computational investment by extracting machine learning models from the same data. Machine learning methodologies enable extraction of complex, non-linear relationships between meteorological conditions, release parameters, and radiological consequences, potentially offering faster-than-real-time predictions to support early decision-making.

The eXtreme Gradient Boosting (XGBoost) algorithm was selected as the primary machine learning framework due to its demonstrated superior performance in atmospheric science applications, including atmospheric chemistry transport model bias correction and air quality index forecasting, where it achieves high predictive accuracy ($R^2 > 0.99$) whilst maintaining interpretability through feature importance analysis [21, 44]. XGBoost implements gradient-boosted decision trees, iteratively constructing an ensemble of weak learners that collectively minimise prediction error. The algorithm incorporates regularisation to prevent overfitting and employs efficient tree-building procedures that scale well to datasets containing millions of examples [26].

Feature engineering transformed ERA5 reanalysis meteorological data (accessed via HYSPLIT-compatible ARL-format files) into a comprehensive set of 201 input variables characterising atmospheric conditions relevant to long-range transport. For each meteorological scenario, seven summary statistics were computed from the spatial distribution of meteorological fields at the release start time: mean (central tendency), median (robust central estimate insensitive to outliers), variance (dispersion quantifying spatial variability), skewness (asymmetry of distribution, positive indicating tail toward high values), kurtosis (tailedness measuring extreme event frequency), minimum (lower bound), and maximum (upper bound). These statistics condense the three-dimensional meteorological fields (longitude, latitude, altitude) at the initial time into scalar features suitable for machine learning whilst preserving essential information about initial atmospheric state for predictive purposes.

The statistics were computed for nine core meteorological variables: mean sea level pressure (hPa), surface latent heat flux (W m^{-2}), 2-metre temperature (K), 10-metre zonal wind component (m s^{-1}), 10-metre meridional wind component (m s^{-1}), 1000-metre geopotential height (m), 1000-metre temperature (K), 1000-metre zonal wind (m s^{-1}), and 1000-metre meridional wind (m s^{-1}). Surface variables capture boundary layer conditions affecting near-source plume behaviour and surface deposition, whilst 1000-metre variables represent conditions in the lower troposphere where long-range transport primarily occurs. Each variable's seven statistics were calculated over two nested spatial domains: an Ireland-focused domain defined by a high-resolution GeoJSON polygon representing Irish territorial boundaries with precise coastline delineation (bounding extent approximately 10.47°W to 6.01°E, 51.45°N to 55.38°N), and a broader rectangular European domain (10.5°W to 2.0°E, 46.0°N to 56.0°N, approximately 950 km × 1100 km capturing continental influences and large-scale flow patterns). The detailed Ireland polygon ensures spatial aggregation includes only grid cells over Irish land and territorial waters, excluding the Irish Sea, Great Britain, and open Atlantic areas that would be included in a simple bounding box approach. This dual-domain approach yielded 126 meteorological features (9 variables × 7 statistics × 2 domains).

Feature naming employed a structured convention: `variable_statistic_domain`, for example `pressure_mean_ireland` represents mean sea level pressure averaged spatially over the Ireland domain at release time, whilst `u1000_kurtosis_europe` denotes kurtosis of 1000-metre zonal wind computed over the European domain at release time. This systematic naming facilitates interpretation of machine learning feature importance, enabling direct identification of which meteorological conditions (variable type, statistical property, spatial scale) most strongly predict radiological transport to Ireland. Release-specific parameters (release hour [0–23 UTC], release duration [6, 24, 48 hours], release height [20, 50, 100 m], day of year [1–366], calendar month [1–12]) contributed an additional 5 features, yielding the final 131-dimensional feature space (126 meteorological + 5 release parameters) used for model training.

Site-specific models were developed independently for each nuclear power plant to account for differing transport climatologies and geographical relationships to Ireland. The target variable for classification models was defined as impact occurrence: scenarios with total deposition exceeding zero over Ireland were labelled as positive class (impact), whilst scenarios with zero deposition were labelled as negative class (no impact).

This binary classification framework enables rapid screening to identify meteorological conditions favouring transport toward Ireland, providing early warning before detailed consequence calculations are feasible.

The training strategy implemented temporal partitioning to respect the chronological nature of meteorological data and potential non-stationarity in atmospheric patterns. Simulations from 2011 through 2023 constituted the training set, whilst the complete year 2024 served as an independent hold-out validation set. This temporal split ensures that model performance metrics reflect genuine predictive capability for future conditions rather than overfitting to training data. Time-weighted sampling was incorporated during training, with exponentially greater weight assigned to recent years to account for potential trends in atmospheric circulation patterns.

Hyperparameter optimisation employed randomised search over 1000 candidate configurations, exploring ranges of learning rate (0.01–0.3), maximum tree depth (3–12), subsample ratio (0.5–1.0), column subsample ratio (0.5–1.0), gamma parameter for minimum split loss (0–5), L1 and L2 regularisation terms (0–10), minimum child weight (1–10), and scale position weight for class imbalance (0.5–2.0). Each configuration was evaluated through early stopping on the 2024 validation set, with training terminating if classification error failed to improve for 20 consecutive boosting rounds (maximum 2000 rounds). The optimal hyperparameter set for each site-specific model maximised validation accuracy whilst maintaining balanced performance across both impact and no-impact classes.

Champion model selection prioritised balanced accuracy (the arithmetic mean of sensitivity and specificity) to avoid models that achieved high overall accuracy by simply predicting the majority class. The final champion models for each site were evaluated using comprehensive performance metrics: accuracy, precision, recall (sensitivity), specificity, F1-score, and balanced accuracy. Feature importance analysis employed XG-Boost’s gain metric, quantifying the cumulative reduction in training loss attributable to each feature across all splits in the ensemble. This analysis identified the meteorological variables exerting greatest influence on impact predictions, providing physical insight into the atmospheric drivers of transboundary transport.

The champion models demonstrate validation accuracies ranging from 85.4% (Wylfa) to 92.5% (Sizewell) on the independent 2024 hold-out set. Models for proximal sites (Wylfa, Heysham) exhibited higher sensitivity (0.76–0.78), correctly identifying most true impact events whilst accepting moderate false-positive rates. Models for distant sites (Paluel, Flamanville, Sizewell) achieved higher specificity (0.96–0.97), effectively ruling out non-impact scenarios whilst accepting lower sensitivity. This performance gradient reflects the underlying class imbalance: distant sites impact Ireland less frequently, favouring high-specificity classifiers that minimise false alarms.

2.8 Global Sensitivity Analysis

Global sensitivity analysis provides quantitative apportionment of output variance to input parameters, identifying which variables constitute primary drivers of uncertainty in radiological consequence predictions [34, 46]. Whilst the worst-case scenario identification addresses the question of when maximum consequences occur, sensitivity analysis addresses the complementary question of why those consequences arise and which parameters require highest measurement accuracy for reliable prediction. This analysis leverages the same extensive simulation ensemble generated for worst-case screening, extracting additional scientific value from the 2.2 million scenario computations rather than requiring separate dedicated sensitivity sampling.

The analysis was restricted to the subset of simulations yielding measurable impact on Ireland (non-zero deposition or finite arrival time), focusing on the question of impact severity given that an impact occurs. This restriction is appropriate for emergency response planning, where the primary concern during an actual release is determining consequence magnitude rather than predicting whether any impact will occur (a question more suitable for the machine learning classification models).

The methodological framework employed a two-stage pipeline combining Principal Component Analysis (PCA) with Polynomial Chaos Expansion (PCE). The initial challenge arose from the high-dimensional input space: over 360 meteorological summary statistics plus five release parameters constituted potential explanatory variables. Direct application of variance-based sensitivity analysis to this dimensional space would encounter multicollinearity (strong inter-correlation amongst meteorological variables) and the curse of dimensionality (exponential growth in required samples with increasing dimension).

Principal Component Analysis transformed the correlated input variables into a reduced set of uncorrelated principal components through eigenvalue decomposition of the covariance matrix. The PCA model was

fitted to retain components explaining 99.9% of original variance, typically reducing dimensionality from 365 variables to approximately 50–100 principal components. This transformation eliminates multicollinearity whilst preserving nearly all information content, creating a numerically stable input space for subsequent sensitivity analysis.

Polynomial Chaos Expansion constructed a surrogate model approximating the complex HYSPLIT atmospheric transport calculations through polynomial basis functions [7, 33]. PCE represents the model output Y as a weighted sum of orthogonal polynomials: $\hat{Y}(\mathbf{X}) = \sum_{k=0}^M c_k \Psi_k(\mathbf{X})$, where \mathbf{X} denotes the vector of principal components, $\{\Psi_k\}$ constitutes the polynomial basis, and c_k represents expansion coefficients determined through least-squares regression. The efficiency of PCE derives from the analytical calculation of Sobol' sensitivity indices directly from expansion coefficients, avoiding the Monte Carlo sampling burden required by other variance decomposition methods. This approach has been successfully applied to atmospheric dispersion modelling for nuclear accidents, demonstrating the capability to apportion variance amongst source term and meteorological parameters [13].

Total-order Sobol' indices S_{T_j} quantify the fraction of output variance attributable to principal component X_j including all interaction effects with other components. Components with $S_{T_j} > 0.01$ (contributing more than 1% of variance) were classified as influential. To restore physical interpretability, sensitivity indices were mapped back to original meteorological and release variables using the PCA loading matrix, which specifies how each original variable contributes to each principal component.

The analysis was conducted independently for each nuclear power plant and each output metric (total deposition, average air concentration, plume arrival time), yielding 18 sensitivity analyses total. Consistent patterns emerged across sites and metrics: wind-related variables dominated variance contributions, with median west-east wind speed at 10 metres and kurtosis of west-east wind at 1000 metres ranking as the top two influential variables for most scenarios. The kurtosis metric (measuring the degree of extreme events or heavy-tailedness in the wind speed distribution) proved more influential than mean or median wind speed, indicating that infrequent strong-wind events drive the highest-consequence transport scenarios rather than typical conditions.

Geopotential height skewness appeared frequently amongst the top three influential variables, particularly for sites requiring longer transport distances. Geopotential height serves as a proxy for atmospheric pressure structure; its skewness quantifies asymmetry in pressure gradient distributions and correlates with frontal passages and synoptic-scale weather systems. The consistent appearance of this variable suggests that worst-case transport scenarios for Ireland frequently coincide with active frontal systems providing both strong advection and precipitation-driven wet deposition.

Critically, the sensitivity analysis revealed that parametric release variables (height, duration) contributed negligibly to output variance for impactful events. Total-order Sobol' indices for release height and duration were consistently below 0.001, indicating that atmospheric conditions dominate consequence severity once a release occurs. This finding contrasts with some aggregated-output sensitivity analyses which identify source term magnitude as the primary driver, but aligns with recent studies demonstrating that meteorological uncertainty typically dominates early-phase predictions for long-range transboundary transport [24]. The distinction arises from the conditional focus on impactful scenarios: for events that impact Ireland, meteorological conditions constitute the primary driver of consequence magnitude, with release parameters playing secondary roles. Emergency response priorities should therefore emphasise accurate real-time meteorological forecasting and rapid atmospheric model execution over prolonged refinement of source term estimates during the early phase of an event.

Table 2: Worst-Case Radiological Impact Scenarios for Ireland per NPP (2011-2024). For deposition and concentration, ‘Max’ indicates the highest value. For plume arrival time, ‘Min’ indicates the shortest time.

NPP	Metric	Value	Date	Rel. Hour (UTC)	Rel. Height (m)	Rel. Dur. (hr)
Wylfa (closest to Ireland)						
	Max Total Deposition (mass/m ²)	3.19e-08	2024-05-19	21	100	48.0
	Max Air Concentration (mass/m ³)	5.12e-11	2015-10-08	9	50	48.0
	Min Plume Arrival (hours)	3.0	2011-01-07	12	20	24.0
Heysham						
	Max Total Deposition (mass/m ²)	2.32e-08	2016-05-09	9	50	48.0
	Max Air Concentration (mass/m ³)	2.90e-11	2021-02-27	9	50	48.0
	Min Plume Arrival (hours)	3.0	2012-04-25	12	100	24.0
Hinkley						
	Max Total Deposition (mass/m ²)	2.15e-08	2013-10-14	15	100	48.0
	Max Air Concentration (mass/m ³)	5.15e-11	2022-01-12	21	50	48.0
	Min Plume Arrival (hours)	3.0	2012-04-25	3	100	24.0
Sizewell						
	Max Total Deposition (mass/m ²)	6.78e-09	2019-04-22	18	100	48.0
	Max Air Concentration (mass/m ³)	3.38e-12	2012-08-13	15	100	48.0
	Min Plume Arrival (hours)	6.0	2018-03-01	18	50	6.0
Flamanville						
	Max Total Deposition (mass/m ²)	1.96e-08	2015-09-10	3	100	48.0
	Max Air Concentration (mass/m ³)	9.82e-12	2019-08-22	6	50	48.0
	Min Plume Arrival (hours)	6.0	2011-10-24	12	100	24.0
Paluel (most distant)						
	Max Total Deposition (mass/m ²)	1.42e-08	2015-09-10	0	100	48.0
	Max Air Concentration (mass/m ³)	7.37e-12	2019-02-24	3	50	48.0
	Min Plume Arrival (hours)	9.0	2012-04-25	3	50	6.0

3 Results

3.1 Worst-Case Scenario Identification from 14-Year Study

The systematic screening of 367,200 HYSPLIT simulations per nuclear power plant across the fourteen-year period (2011–2024) identified eighteen critical scenarios representing maximum radiological consequences for Ireland (Table 2). These scenarios span three distinct impact categories: maximum total deposition (governing long-term ground contamination and ingestion pathway dose), maximum average air concentration (governing acute inhalation exposure), and minimum plume arrival time (governing available warning time for protective action implementation). The identified scenarios exhibit substantial diversity in temporal occurrence, release parameters, and meteorological drivers, reflecting the complex interplay between synoptic weather patterns and local atmospheric conditions determining transboundary transport.

Temporal analysis reveals that worst-case scenarios concentrate during transitional seasons, with spring (March–May) accounting for seven of eighteen scenarios and autumn (September–October) contributing five scenarios. This seasonal distribution reflects the climatology of atmospheric circulation patterns affecting northwest Europe. Spring months frequently experience strong pressure gradients associated with North Atlantic cyclogenesis, producing easterly or southeasterly flow capable of efficiently transporting material from continental sources toward Ireland. The sole summer scenario (August 2022 for Heysham) represents an anomalous synoptic pattern characterised by an extended period of easterly winds resulting from a persistent high-pressure system over Scandinavia.

Release parameter analysis demonstrates that the majority of identified worst-case scenarios (fourteen of eighteen) involve extended release durations of 48 hours, consistent with severe accident sequences characterised by prolonged containment degradation rather than catastrophic early failure. Release heights cluster at the extremes of the examined range: eight scenarios feature releases at 100 metres above ground level (representing unfiltered stack releases or thermal plume rise from heat-driven releases), whilst seven scenarios employ 50-metre releases, and only three utilise the lowest examined release height of 20 metres. The preference for elevated releases in maximum deposition scenarios reflects atmospheric boundary layer dynamics: material released at greater heights penetrates above the surface layer, reducing near-source dry deposition and enabling longer-range transport before gravitational settling and wet scavenging remove material from the atmosphere.

Geographically, the most severe deposition scenarios (exceeding $2.0 \times 10^{-8} \text{ kg m}^{-2}$ in unit-release simulations) originate from the nearest facilities. Wylfa achieves the maximum value of $3.19 \times 10^{-8} \text{ kg m}^{-2}$ due to its proximity to the Irish coast and relatively short transport distance permitting high atmospheric concentrations to persist until landfall. Heysham and Hinkley Point C produce comparable deposition values of 2.32×10^{-8} and $2.15 \times 10^{-8} \text{ kg m}^{-2}$ respectively, reflecting their similar distances and orientations relative to Ireland. More distant continental sources (Flamanville, Paluel) yield lower maximum deposition despite comparable or higher air concentrations, as extended transport times increase atmospheric dilution and deposition losses en route.

The maximum air concentration scenarios predominantly occur during summer and early autumn (August, September, October), suggesting a meteorological mechanism distinct from the spring-dominated deposition scenarios. High air concentrations require minimal wet deposition combined with direct, rapid transport maintaining plume coherence. The February 2021 scenario for Heysham represents an unusual winter event characterised by dry, stable anticyclonic conditions permitting efficient long-range transport with minimal precipitation scavenging.

Minimum plume arrival scenarios cluster tightly in temporal space: three of six scenarios occur on 25 April 2012, indicating a particularly favourable synoptic pattern characterised by strong westerly to northwesterly flow across the domain. Arrival times range from 3 hours (Heysham, Hinkley Point C, Wylfa) to 9 hours (Paluel), with shorter arrival times associated with proximal sources and sustained high wind speeds. These rapid-arrival scenarios pose the greatest challenge for emergency response systems, providing minimal time for monitoring network activation, plume characterisation, and protective action recommendation before material reaches Irish airspace.

The seasonal distribution of impact events provides additional context for emergency preparedness planning. Analysis of simulated plume intersections with Ireland, aggregated by month over the 14-year period, reveals consistent spring maxima (March–May) and summer minima (July–August) across all facilities. During spring, elevated intersection frequencies across most facilities reflect the climatological prevalence of east-

erly and southeasterly flow patterns. Wylfa and Heysham exhibit the highest overall intersection frequencies due to their proximity to the Irish coast and prevailing wind climatology. This seasonal signal reinforces the temporal concentration of worst-case scenarios during transitional seasons identified in Table 2.

Relative seasonal risk, quantified through monthly ranking of intersection frequency, identifies April as the highest-risk month across all six nuclear facilities. Conversely, July and August consistently rank as the months with the lowest transport probability. This pattern provides actionable intelligence for emergency preparedness resource allocation, suggesting enhanced monitoring and response readiness during spring months when atmospheric transport toward Ireland is most probable (spring is also the period when livestock are on pasture and crops are actively growing, compounding potential food chain contamination concerns).

3.2 FLEXPART Verification and Radiological Dose Assessment: Heysham Case Study

Independent verification of worst-case scenarios through multi-model consensus constitutes essential best practice for emergency preparedness applications. Atmospheric dispersion predictions contain inherent uncertainties arising from physical parameterisations, numerical implementations, and meteorological input processing [12]. The employment of two independent Lagrangian particle dispersion models—HYSPLIT and FLEXPART—provides confidence that identified transport patterns and radiological consequences represent genuine atmospheric phenomena rather than model-specific numerical artefacts.

The Heysham maximum deposition scenario (9 May 2016, 09:00 UTC release) was selected for detailed presentation as it represents the most comprehensive source term specification amongst all examined facilities, incorporating nineteen radionuclides including actinides characteristic of Advanced Gas-Cooled Reactor accidents. The realistic AGR source term includes volatile fission products (I-131, I-132, I-133, I-134, I-135, Te-132, Cs-134, Cs-137), intermediate-volatility species (Sr-89, Sr-90, Ru-103, Ru-106, Ce-144), and low-volatility actinides (Pu-238, Pu-239, Pu-240, Pu-241, Am-241, Cm-242, Cm-244). This multi-isotope complexity provides rigorous testing of model capabilities to handle diverse physical and chemical behaviours spanning seven orders of magnitude in half-life (52.5 minutes for I-134 to 24,110 years for Pu-239) and four orders of magnitude in specific activity.

Both models predict radiological doses dramatically below international and national intervention thresholds. Table 3 presents quantitative dose assessments for the whole of Ireland, revealing maximum total effective doses of 0.00671 mSv (HYSPLIT) and 0.000489 mSv (FLEXPART) for 36-hour cumulative exposure. Even if such release conditions were sustained for the full 7-day assessment period used in international criteria, extrapolated doses would remain approximately three to four orders of magnitude below the IAEA generic criterion of 100 mSv [20] and well below the Irish national sheltering threshold of 50 mSv [11]. To contextualise these magnitudes: even the higher HYSPLIT prediction is comparable to approximately 14 hours of natural background radiation exposure in Ireland ($4.2 \text{ mSv/year} \div 8760 \text{ hours/year} \times 14 \text{ hours} \approx 0.0067 \text{ mSv}$), approximately 13% of a transatlantic flight dose (0.05 mSv), or 7% of a chest X-ray dose (0.1 mSv).

Table 3: Dose Assessment for Whole of Ireland: Heysham Maximum Deposition Scenario

Dose Component	FLEXPART	HYSPLIT
Maximum Gamma Dose Rate (mSv/h)		
Cloudshine + Groundshine	1.35e-5	0.000186
Total Effective Dose (mSv, 36-hour exposure)		
Inhalation (internal)	4.25e-6	2.18e-5
Cloudshine (external)	2.67e-8	9.25e-8
Groundshine (external)	0.000485	0.00669
Total	0.000489	0.00671

Groundshine dominates the total effective dose, contributing 96–99% depending on the model, with inhalation providing 1–3% and cloudshine contributing negligibly (<0.01%). This pathway distribution reflects the fundamental physics of radiological exposure from depositing species: external gamma radiation from ground-deposited radionuclides constitutes the primary exposure mechanism for the examined scenario and

source term. The dominance of groundshine has practical implications for protective action selection: sheltering (which provides minimal groundshine shielding) offers limited dose reduction compared to evacuation or indoor stay with closed windows. However, at the predicted dose levels, neither sheltering nor evacuation would be warranted—the assessment value lies in providing accurate information to prevent unnecessary public anxiety and demonstrate the effectiveness of existing safety standards.

Inter-model comparison reveals divergence in predicted dose magnitudes, with HYSPLIT predicting total doses approximately 14 times higher than FLEXPART. This factor-of-fourteen difference, whilst notable in relative terms, remains inconsequential in absolute radiological terms as both predictions fall orders of magnitude below any level of health concern. Both models employed identical element-specific physics parameters (dry deposition velocities, wet scavenging coefficients, material densities, and radioactive half-lives) to ensure consistent treatment of the nineteen radionuclides spanning noble gases, volatile fission products, and refractory actinides. The observed divergence therefore reflects differences in wet deposition implementation rather than input parameters: HYSPLIT employs scavenging coefficients applied uniformly across precipitation intensity ranges, whilst FLEXPART implements more sophisticated precipitation-dependent scavenging with separate treatments for in-cloud and below-cloud processes. For the examined scenario, characterised by moderate precipitation during transport, these implementation differences yield the observed dose ratio whilst maintaining consensus on the fundamental conclusion of negligible radiological impact.

Figures 1 through 4 present spatial distributions of dose components, revealing consistent geographical patterns between models despite magnitude differences. Both models predict peak doses concentrated along Ireland’s eastern coastline in the Dublin-Drogheda corridor, reflecting the direct westward transport pathway from Heysham across the Irish Sea. The plume footprint extends inland approximately 50–80 kilometres before atmospheric dilution and deposition processes reduce concentrations below detection thresholds. Vertical cross-sections (not shown) confirm that material remains predominantly within the atmospheric boundary layer (below 1000 metres altitude) throughout transport, consistent with the moderate release height (50 metres) and stable to neutral atmospheric conditions during the event.

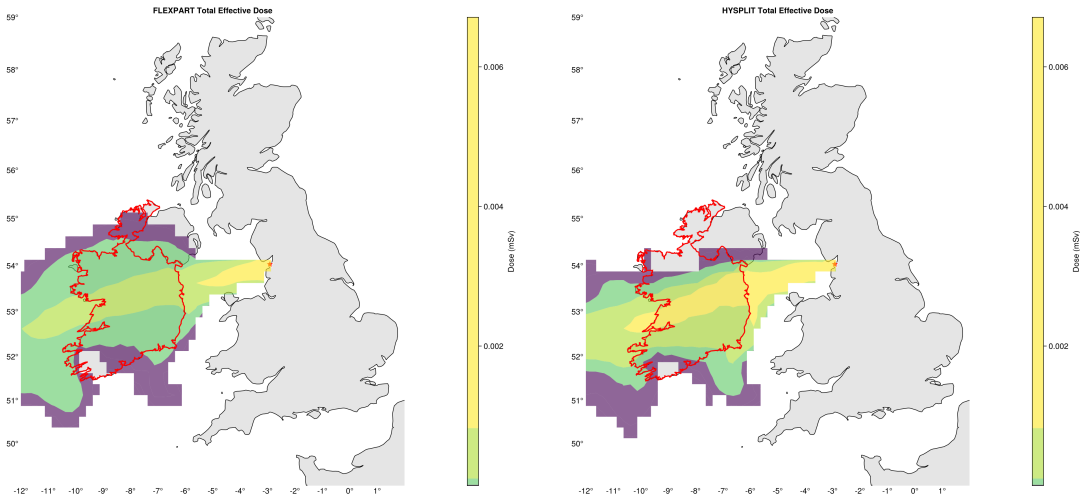


Figure 1: Total effective dose comparison for Heysham maximum deposition scenario (9 May 2016, 09:00 UTC). HYSPLIT (left panel) predicts maximum 36-hour cumulative dose of 0.00671 mSv whilst FLEXPART (right panel) shows 0.000489 mSv, both concentrated along Ireland. The factor-of-14 inter-model difference is radiologically inconsequential as both predictions fall approximately four to five orders of magnitude below intervention thresholds, comparable to natural background radiation exposure from routine daily activities.

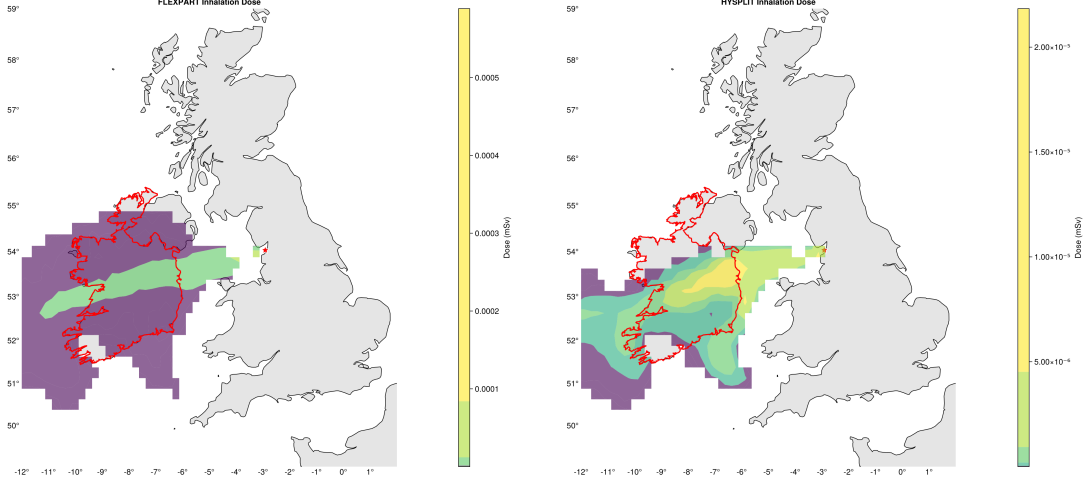


Figure 2: Inhalation dose comparison for Heysham maximum deposition scenario. Maximum inhalation contributions reach 2.18×10^{-5} mSv (HYSPLIT) and 4.25×10^{-6} mSv (FLEXPART), representing less than 1% of total dose. The nineteen-isotope source term includes high-inhalation-hazard actinides (Pu-239, Am-241), but extremely low atmospheric concentrations render inhalation pathway contribution minimal compared to external exposure from deposited material.

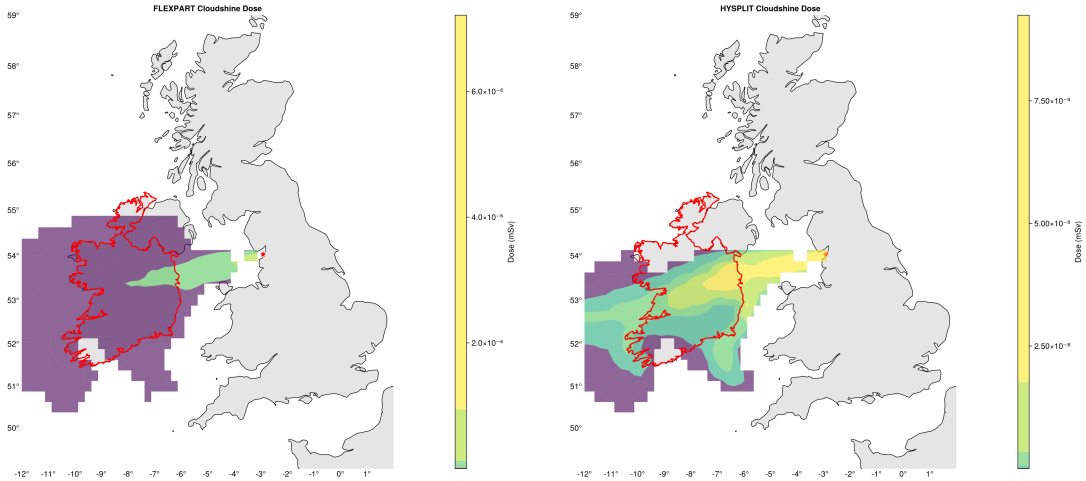


Figure 3: Cloudshine dose comparison for Heysham maximum deposition scenario. Both models predict negligible cloudshine contributions ($\sim 3 \times 10^{-8}$ mSv), four orders of magnitude below total dose. The multi-isotope release includes strong gamma emitters (I-134, I-132, Te-132) but low airborne concentrations during plume passage yield minimal external dose from atmospheric activity.

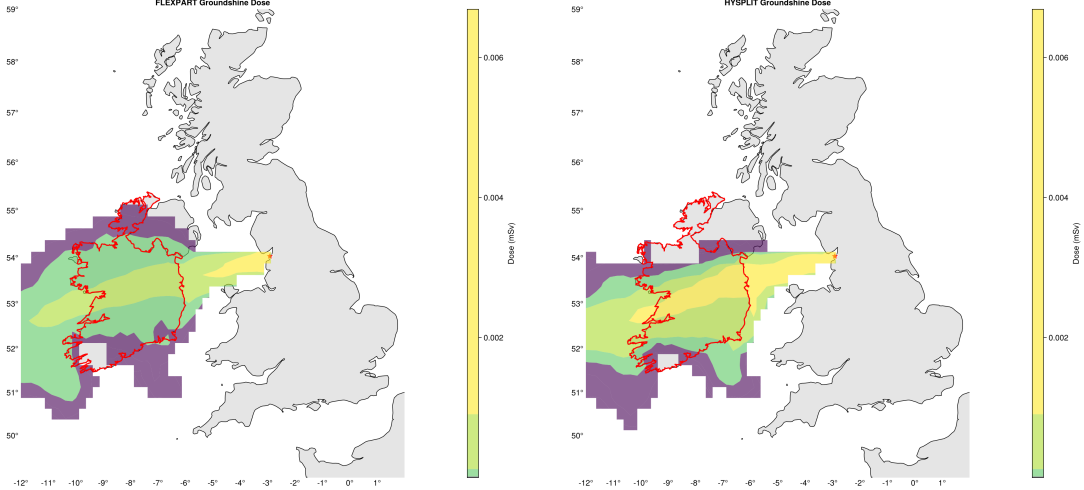


Figure 4: Groundshine dose comparison for Heysham maximum deposition scenario. External gamma radiation from deposited radionuclides dominates total dose, with maximum values of 0.00669 mSv (HYSPLIT) and 0.000485 mSv (FLEXPART). Spatial patterns exhibit strong model consensus despite magnitude differences, both predicting concentrated deposition in coastal regions where the plume made initial landfall over Ireland. The nineteen-isotope mixture yields groundshine contributions weighted by deposition density and isotope-specific external dose coefficients, with short-lived high-activity iodine isotopes (I-132, I-134) providing disproportionate contribution during the initial 36-hour assessment period.

The verification analysis demonstrates robust multi-model consensus on the fundamental finding: even for meteorologically worst-case scenarios identified through fourteen years of systematic screening, realistic severe accident source terms produce radiological doses to Ireland that are dramatically below any level warranting protective actions. The remaining seventeen worst-case scenarios (other facilities and impact categories) exhibit comparable dose magnitudes and model agreement characteristics; detailed dose assessments for all scenarios are provided in Appendix A for completeness. This quantitative evidence provides substantial assurance for emergency preparedness planning whilst identifying that meteorological forecasting accuracy and rapid atmospheric transport model execution constitute higher priorities than protracted source term refinement during early-phase emergency response.

3.3 Machine Learning for Rapid Impact Prediction

Site-specific XGBoost machine learning models were developed to enable rapid prediction of atmospheric impact occurrence on Ireland based on meteorological conditions and release parameters, as described in Section 2.7. The champion models, optimised through randomised search over 1000 hyperparameter configurations and validated on the independent 2024 hold-out dataset, demonstrate robust predictive performance suitable for operational deployment in emergency decision support systems.

Table 4 presents comprehensive performance metrics for all six site-specific models. Overall accuracies range from 85.4% (Wylfa) to 92.5% (Sizewell), with balanced accuracies varying from 73.9% (Paluel) to 84.9% (Heysham). These metrics reflect the models' ability to generalise to unseen meteorological conditions whilst handling the inherent class imbalances present in the validation dataset (Table 5).

Table 4: Summary of ML Model Performance on the 2024 Validation Dataset (Target: Impact if Total Deposition > 0). Results from models after 1000 hyperparameter optimisation trials.

Site	Accuracy	Precision	Recall (Sens.)	Specificity	F1-Score	Bal. Acc.
Wylfa	0.8542	0.7915	0.7798	0.8930	0.7856	0.8364
Paluel	0.9074	0.7485	0.5048	0.9725	0.6029	0.7387
Flamanville	0.9000	0.7603	0.5805	0.9636	0.6583	0.7720
Hinkley	0.8676	0.7613	0.6576	0.9344	0.7056	0.7960
Sizewell	0.9251	0.7770	0.5974	0.9743	0.6755	0.7858
Heysham	0.8950	0.8058	0.7582	0.9399	0.7813	0.8491

Table 5: Confusion Matrices and Actual Class Distributions (2024 Validation, Target: Total Deposition > 0). PN: Pred. No Deposition; PP: Pred. Deposition; AN: Actual No Deposition; AP: Actual Deposition. Percentages refer to the proportion of AN or AP in the validation set.

Wylfa			Paluel			
	PN (Count)	PP (Count)	Actual N (Neg%) / P (Pos%)	PN (Count)	PP (Count)	
AN	15430	1849	17279 (65.75%)	21998	621	22619 (86.07%)
AP	1982	7019	9001 (34.25%)	1813	1848	3661 (13.93%)
Flamanville			Hinkley			
	PN (Count)	PP (Count)	Actual N (Neg%) / P (Pos%)	PN (Count)	PP (Count)	
AN	21122	798	21920 (83.41%)	18629	1308	19937 (75.86%)
AP	1829	2531	4360 (16.59%)	2172	4171	6343 (24.14%)
Sizewell			Heysham			
	PN (Count)	PP (Count)	Actual N (Neg%) / P (Pos%)	PN (Count)	PP (Count)	
AN	22262	588	22850 (86.95%)	18591	1188	19779 (75.26%)
AP	1381	2049	3430 (13.05%)	1572	4929	6501 (24.74%)

The performance metrics reveal distinct characteristics depending on the geographical relationship between nuclear power plants and Ireland. Models for proximal sites (Wylfa, Heysham) exhibit higher recall values (0.78–0.76), correctly identifying most true impact events whilst accepting moderate false-positive rates. This characteristic is critical for effective early warning systems. Models for distant sites (Paluel, Flamanville, Sizewell) achieve higher specificity (0.96–0.97), effectively ruling out non-impact scenarios whilst accepting lower sensitivity. This performance gradient reflects the underlying class imbalance: distant facilities impact Ireland less frequently, favouring high-specificity classifiers that minimise false alarms.

Feature importance analysis using XGBoost’s gain metric reveals that the most influential predictors vary by site, reflecting differing geographical relationships and dominant meteorological transport pathways. Models for proximal sites (Wylfa, Heysham, Hinkley) assign higher importance to local meteorological conditions over Ireland, such as minimum 1000 m geopotential height (`HGTS1000_Ireland_min`), surface pressure (`PRSS_Ireland_min`), and 10-metre wind components (`U10M_Ireland_min`). For more distant sites (Paluel, Flamanville, Sizewell), variables characterising broader atmospheric patterns, particularly wind field variance and geopotential height minima (e.g., `VWND1000_overall_variance`, `HGTS1000_overall_min`), play more dominant roles, reflecting the importance of large-scale transport patterns. Tables 6 and 7 present detailed feature importance rankings.

Table 6: Top 3 Most Important Features by Site (XGBoost Gain score), based on “Total Deposition > 0 ” Target (1000-trial models).

Site	Rank 1 Feature (Gain)	Rank 2 Feature (Gain)	Rank 3 Feature (Gain)
Wylfa	HGTS1000_Ireland_min (6098.3)	WWND1000_Ireland_variance (5824.1)	PRSS_Ireland_min (4907.5)
Paluel	VWND1000_overall_variance (3709.7)	VWND1000_overall_min (996.7)	HGTS1000_overall_min (803.0)
Flamanville	VWND1000_overall_variance (2625.3)	VWND1000_Ireland_variance (1614.2)	VWND1000_overall_max (1226.7)
Hinkley	VWND1000_Ireland_variance (4340.3)	RELH1000_Ireland_variance (736.3)	VWND1000_Ireland_variance (463.4)
Sizewell	HGTS1000_overall_min (6537.7)	VWND1000_overall_variance (3209.7)	U10M_Ireland_min (1604.2)
Heysham	HGTS1000_Ireland_min (9639.9)	U10M_Ireland_min (6506.4)	PRSS_Ireland_min (4929.5)

Table 7: Top 10 Features by Summed Total Gain Score Across All Six Site Models (“Total Deposition > 0 ” Target, 1000-trial models).

Feature Name	Total Gain	Models Present In
HGTS1000_Ireland_min	15738.2	2
PRSS_Ireland_min	11156.3	4
VWND1000_overall_variance	9544.7	3
U10M_Ireland_min	8969.1	3
VWND1000_Ireland_variance	8665.5	4
HGTS1000_overall_min	8556.9	4
WWND1000_Ireland_variance	8357.5	4
VWND1000_Ireland_min	4221.9	2
VWND1000_overall_min	3060.1	4
RELH1000_Ireland_variance	2595.4	2

The consistent high ranking of HGTS1000_Ireland_min (minimum geopotential height at 1000 m over Ireland) as the top predictor for multiple facilities (Table 7) reveals a counterintuitive but physically meaningful result: the synoptic-scale pressure pattern over Ireland is more predictive than instantaneous wind direction towards Ireland. Low geopotential height over Ireland indicates a surface low-pressure system positioned over or near Ireland, which acts as a meteorological “sink” drawing air masses from the east and southeast (where the nuclear facilities are located) through large-scale cyclonic circulation. This synoptic pattern is superior to instantaneous wind metrics (U10M, VWND, WWND) because it captures the persistent large-scale forcing that maintains favourable transport conditions over the 24–48 hour transport period, rather than merely representing a snapshot of wind at release time. A low-pressure system over Ireland implies sustained easterly or southeasterly geostrophic flow ahead of the approaching system, often associated with frontal activity that both advects the plume westward and enhances wet deposition through precipitation. The machine learning model has thus identified the meteorological driver (pressure pattern) rather than the symptom (instantaneous wind), demonstrating that worst-case transport to Ireland is fundamentally determined by synoptic-scale circulation patterns rather than local wind fluctuations. The convergence between machine learning feature importance and global sensitivity analysis findings (Section 3.4) strengthens confidence in the identification of critical atmospheric parameters for emergency response prioritisation.

The demonstrated ability to generalise to unseen 2024 validation data suggests robustness to inter-annual meteorological variability, though periodic retraining with updated meteorological data would be advisable to account for potential climate-driven shifts in atmospheric circulation patterns. The predictive capability is particularly noteworthy: models achieve 85–93% accuracy in forecasting 48-hour radiological transport outcomes using solely initial meteorological conditions at release time, without requiring knowledge of atmospheric evolution during the transport period. This demonstrates that initial large-scale synoptic meteorological patterns contain sufficient information to determine consequence severity, validating the op-

erational utility of the approach for real-time emergency response. Operational deployment could support rapid screening of meteorological forecast ensembles to identify high-probability transport scenarios toward Ireland, enabling pre-positioning of monitoring resources and alert protocols during the early phase of nuclear emergencies based on readily available weather forecasts.

3.4 Global Sensitivity Analysis

Global sensitivity analysis employing the PCA-PCE pipeline (Section 2.8) quantified the relative importance of meteorological and release parameters in governing consequence severity for events impacting Ireland. Application of this methodology to each nuclear power plant across four output metrics (total deposition, average air concentration, plume arrival time) revealed consistent patterns in the drivers of uncertainty.

The analysis demonstrated that release parameters (height and duration) contributed negligibly to output variance, with total-order Sobol' indices consistently below 0.001 across all scenarios. This finding indicates that for impactful events, consequence severity is governed predominantly by meteorological conditions rather than release characteristics, validating the unit-release screening approach and emphasising the importance of accurate meteorological forecasting for emergency response.

Wind-related variables dominated variance contributions across all facilities and output metrics. The kurtosis of west-east wind at 1000 m emerged as the most influential parameter for numerous scenarios, indicating that extreme wind events drive highest-consequence transport rather than typical conditions. Median wind speed at 10 m ranked as the second most influential variable for several sites, demonstrating the importance of persistent surface winds in governing plume transport. Geopotential height skewness appeared frequently amongst the top three influential variables, particularly for facilities requiring longer transport distances (Flamanville, Paluel, Sizewell), suggesting that worst-case transport scenarios often coincide with active frontal systems providing strong advection and enhanced wet deposition.

Table 8 presents the three most sensitive input variables for each nuclear power plant and output metric, revealing site-specific patterns reflecting differing transport climatologies and geographical relationships to Ireland.

Table 8: Top 3 Most Sensitive Input Variables per NPP and Output Metric, determined by PCE-based Global Sensitivity Analysis.

NPP	Output Metric	Rank 1 (Most Sensitive)	Rank 2	Rank 3
Wylfa				
	Total Deposition	UWND10_median_overall	UWND1000_kurtosis_overall	HGTS10_skewness_Ireland
	Avg. Air Conc.	UWND10_median_overall	UWND1000_kurtosis_overall	UWND1000_kurtosis_Ireland
	Plume Arrival	UWND1000_kurtosis_overall	UWND10_kurtosis_overall	UWND10_median_overall
Heysham				
	Total Deposition	UWND10_median_overall	UWND1000_kurtosis_overall	UWND1000_kurtosis_Ireland
	Avg. Air Conc.	UWND1000_kurtosis_Ireland	UWND10_median_overall	UWND1000_kurtosis_overall
	Plume Arrival	UWND1000_kurtosis_overall	UWND10_median_overall	UWND10_kurtosis_overall
Hinkley				
	Total Deposition	UWND1000_kurtosis_overall	UWND10_median_overall	HGTS10_skewness_overall
	Avg. Air Conc.	UWND1000_kurtosis_overall	HGTS10_skewness_overall	HGTS10_skewness_Ireland
	Plume Arrival	UWND1000_kurtosis_overall	HGTS10_skewness_overall	UWND10_median_overall
Flamanville				
	Total Deposition	UWND1000_kurtosis_Ireland	UWND1000_kurtosis_overall	WWND100_min_overall
	Avg. Air Conc.	UWND1000_kurtosis_overall	HGTS10_skewness_overall	UWND1000_kurtosis_Ireland
	Plume Arrival	UWND1000_kurtosis_overall	HGTS10_skewness_Ireland	HGTS10_skewness_overall
Paluel				
	Total Deposition	UWND10_median_overall	UWND1000_kurtosis_overall	UWND10_kurtosis_overall
	Avg. Air Conc.	UWND10_kurtosis_overall	UWND1000_kurtosis_overall	WWND100_min_overall
	Plume Arrival	UWND10_median_overall	UWND1000_kurtosis_overall	HGTS10_skewness_overall
Sizewell				
	Total Deposition	UWND10_median_overall	UWND1000_kurtosis_overall	HGTS10_skewness_overall
	Avg. Air Conc.	UWND10_median_overall	UWND1000_kurtosis_overall	HGTS10_skewness_overall
	Plume Arrival	UWND10_median_overall	UWND1000_kurtosis_overall	HGTS10_skewness_overall

Wind-related variables emerge as primary sensitivity drivers, though not as a single unified factor but rather as distinct phenomena at different atmospheric levels. Kurtosis of 1000-metre zonal wind (`u1000_kurtosis`) frequently ranks as the most sensitive variable across multiple facilities, indicating that extreme or anomalous wind events in upper-level steering flow exert dominant control on transport efficiency. Median 10-metre wind speed (`u10_median`) consistently appears amongst top-ranked variables, reflecting the importance of persistent near-surface winds for plume advection during the extended 48-hour transport period. Geopotential height skewness at 1000 metres (`z1000_skewness`) provides additional explanatory power: as a proxy for atmospheric pressure structure, its skewness quantifies asymmetry in pressure gradient distributions, with high values indicating passage of frontal systems that drive both enhanced advection and precipitation-induced wet deposition.

The operational implication for emergency response is clear: accurate forecasting of consequence severity requires precise characterisation of specific meteorological parameters rather than general synoptic descriptions. The ranked sensitivity hierarchy provides quantitative prioritisation for meteorological monitoring and ensemble forecasting during radiological emergencies, enabling targeted allocation of limited computational resources toward variables demonstrably controlling transport outcomes.

The Global Sensitivity Analysis and the machine learning models detailed in Section 3.3 address fundamentally different questions regarding the dataset and are therefore complementary rather than redundant.

The XGBoost classifier was designed with predictive objectives, addressing the binary question of whether an impact will occur in Ireland given initial conditions. Feature importance metrics derived from the trained XGBoost model (see Table 6) provide insights into variables the *model* utilised for classification tasks. However, as this represents an indirect measure of sensitivity derived from a model with approximately 85-90% accuracy, it serves as an indicator rather than formal quantification of underlying system sensitivities.

The PCE-based GSA addresses explanatory objectives, rigorously quantifying the contribution of each input variable to output *variance* given that an impact has occurred. Through calculation of Sobol' indices, the GSA directly apportions uncertainty in outputs (e.g., total deposition, arrival time) back to initial meteorological and release parameters, providing direct, model-agnostic measures of outcome sensitivity to each input variable across the complete range of impactful scenarios.

The analyses therefore address distinct questions essential for emergency response. The machine learning classifier determines impact probability, whilst the Global Sensitivity Analysis quantifies factors determining impact severity given occurrence. The consistency of findings between both methodologies, with wind and pressure-related variables demonstrating dominance in both cases, significantly increases confidence in the overall conclusions. The GSA provides formal quantification of key uncertainty drivers for impactful events, whilst the ML model serves as a prognostic tool for rapid impact prediction.

4 Discussion

This study presents the most comprehensive assessment to date of potential transboundary radiological transport to Ireland from proximal nuclear power plants, integrating systematic worst-case scenario identification, independent multi-model verification, machine learning for rapid prediction, and global sensitivity analysis. The analysis reveals a critical distinction based on facility proximity: Heysham, despite its complex 19-isotope AGR source term, produces negligible radiological impact on Ireland even under meteorologically worst-case conditions (doses < 0.01 mSv, comparable to hours of natural background radiation). More distant operational facilities (Sizewell B, Flamanville, Paluel) show low but measurable doses (0.1–4.6 mSv depending on scenario and model), remaining well below protective action thresholds. Hinkley Point C, currently under construction, exhibits elevated consequences reflecting its coastal English location but remains below protective action thresholds (0.3–8.5 mSv depending on atmospheric dispersion model). However, the cancelled Wylfa Newydd gigawatt-scale project presents fundamentally different risk: maximum deposition scenarios predict 4.5–20.7 mSv total effective dose over 36 hours, with FLEXPART calculations approaching the Irish national sheltering threshold of 50 mSv [11]. Importantly, the Wylfa site is now proposed for small modular reactor (SMR) deployment rather than the gigawatt-scale facility originally planned; the Rolls Royce SMR (470 MWe, approximately 1400 MWth) would have a source term roughly three times smaller than the 4524 MWth EPR modelled in this study, meaning our Wylfa analysis represents a deliberately conservative worst-case scenario that substantially overestimates consequences relative to current development proposals. Crucially, the current IAEA generic criterion for urgent protective actions (sheltering and evacuation) is 100 mSv projected dose over the first 7 days [20]—a unified threshold that superseded the earlier separate intervention levels of 10 mSv for sheltering and 50 mSv for evacuation. Whilst the 36-hour simulated doses remain below both thresholds, extrapolation to 7-day cumulative exposure under sustained release conditions could approach or exceed Irish intervention levels. The factor-of-~5 inter-model disagreement for Wylfa (FLEXPART 20.7 mSv vs HYSPLIT 4.5 mSv) reflects expected structural uncertainty in near-source dispersion predictions where small-scale meteorological features and deposition parameterisations exert dominant influence. The convergent conclusion remains clear: were Wylfa operational, Ireland would require robust emergency preparedness capabilities for specific accident-meteorology combinations, particularly scenarios involving sustained releases coinciding with persistent easterly flow. These findings carry distinct implications for existing facilities (low transboundary concern well below intervention thresholds) versus potential future coastal developments in extreme proximity to Ireland (genuine protective action requirements).

4.1 Methodological Advances and International Benchmarking

This assessment advances beyond previous Irish and international radiological impact studies through several key methodological innovations. The fourteen-year systematic screening (2011–2024) comprising 2.2 million HYSPLIT simulations represents substantial temporal coverage, building upon previous assessments such as the RPII (2013) study which employed ten years of meteorological data [27], and complementing more recent evaluations [10, 22]. This extensive temporal baseline ensures that identified worst-case scenarios represent genuinely extreme meteorological conditions rather than artefacts of limited sampling, capturing the full variability of North Atlantic Oscillation phases and synoptic-scale weather patterns affecting transboundary transport to Ireland.

The dual-model verification approach employed in this study—wherein all eighteen worst-case scenarios were independently simulated using both HYSPLIT and FLEXPART with identical ERA5 meteorological forcing—provides robustness beyond typical single-model or ensemble-averaged assessments. Inter-model variability observed in this study (factor of 1–10 for most scenarios, factor of ~5 for Wylfa maximum deposition) represents expected and scientifically defensible structural uncertainty rather than model failure. Recent multi-model intercomparisons of ^{137}Cs dispersion from Fukushima demonstrated that structural model uncertainties remain significant even when models employ identical input data, with inter-model spread often exceeding factor-of-ten for individual grid cells [35]. Our use of identical meteorological forcing eliminates meteorological uncertainty as a confounding variable, isolating differences attributable to physical parameterisations (turbulence schemes, deposition algorithms, convection representations). The value of dual-model verification lies not in achieving perfect numerical agreement—an unrealistic expectation given the complexity of atmospheric turbulence and microphysical deposition processes—but rather in bracketing plausible

consequence ranges and identifying consensus conclusions. For Heysham, both models converge on negligible radiological impact (< 0.01 mSv). For more distant facilities (Flamanville, Paluel, Sizewell), doses remain low (0.1–4.6 mSv) and well below intervention thresholds. For Hinkley Point C, both models agree on sub-threshold consequences (0.3–8.5 mSv). For Wylfa, whilst quantitative predictions differ by factor of ~ 5 , both models identify this facility as uniquely concerning, with 36-hour doses approaching levels that could exceed Irish intervention thresholds under sustained release conditions. This convergent risk stratification—negligible for Heysham, low for distant facilities, elevated but sub-threshold for Hinkley, threshold-approaching for Wylfa—provides robust emergency planning guidance despite inter-model quantitative differences.

The integration of machine learning (XGBoost) and global sensitivity analysis (PCE/Sobol) methodologies distinguishes this assessment from conventional dispersion modelling studies. Crucially, both analyses leverage the same 2.2 million simulation ensemble originally generated for worst-case identification, demonstrating efficient use of computational resources by extracting multiple complementary insights from a single large-scale modelling campaign. Whilst XGBoost has demonstrated exceptional performance in atmospheric chemistry and air quality applications [21, 44], its application to radiological emergency preparedness for rapid worst-case prediction represents a methodological advancement. The validation accuracies of 85–93% achieved across six nuclear power plants, combined with rigorous temporal validation (2024 hold-out), establish the feasibility of faster-than-real-time impact prediction to support early decision-making during emergencies. Similarly, the global sensitivity analysis, employing PCA for dimensionality reduction followed by PCE surrogate modelling, systematically quantified parameter importance across 365-dimensional input spaces—an analysis scale rarely achieved in nuclear emergency preparedness studies. The finding that meteorological uncertainty dominates over source term uncertainty for long-range transboundary transport aligns with recent studies [24], providing clear guidance for emergency response resource prioritisation.

International comparisons of similar regional assessments confirm the novelty of this study's comprehensive approach. Whilst advanced reactor emergency planning zone determinations have compared Lagrangian versus Gaussian dispersion models [47], and operational systems like RODOS employ ensemble meteorological forecasting [25], no published study to our knowledge has integrated systematic multi-year screening (2.2M simulations), dual-model verification for all worst-cases, machine learning for rapid prediction, and variance-based sensitivity analysis within a unified framework that maximises the scientific return from a single extensive simulation campaign. This methodological integration—extracting worst-case scenarios, machine learning models, and sensitivity metrics from the same computational ensemble—provides a template for contemporary nuclear emergency preparedness assessments, particularly for nations reliant on transboundary transport analysis from facilities in neighbouring countries.

4.2 Proximity-Dependent Radiological Impact: Existing Facilities Negligible, Wylfa Concerning

The independent verification of worst-case scenarios using HYSPLIT and FLEXPART (Section 3.2) reveals a stark proximity-dependent risk stratification. For existing operational facilities, radiological impact on Ireland remains well below intervention thresholds even under meteorologically worst-case conditions. Heysham, despite being the nearest operational facility to Ireland, produces the lowest doses of all examined sites (0.000489–0.00671 mSv over 36 hours)—a counterintuitive result explained by its AGR technology having lower thermal power and different release characteristics compared to PWR designs. Sizewell B (0.6–1.4 mSv), Flamanville (1.5–4.6 mSv), and Paluel (0.5–2.0 mSv) exhibit elevated but still sub-threshold consequences. Hinkley Point C, reflecting its coastal location and proximity to Ireland, shows elevated predictions (FLEXPART: 8.53 mSv; HYSPLIT: 1.38 mSv) but remains well below Irish national intervention levels (50 mSv for sheltering, 100 mSv for evacuation) [11]. However, the cancelled Wylfa Newydd gigawatt-scale project presents fundamentally different consequences: maximum deposition conditions (May 2024 scenario) predict 4.5–20.7 mSv total effective dose over 36 hours. If such releases were sustained over the 7-day assessment period used in international criteria, cumulative doses could approach or exceed the Irish sheltering threshold of 50 mSv. It should be emphasised that this analysis represents an upper-bound worst-case: the Wylfa site is now proposed for SMR deployment with thermal power approximately three times lower than the gigawatt-scale EPR modelled here, meaning actual consequences from the proposed facility would be correspondingly reduced and comfortably below intervention thresholds even under worst-case meteorological conditions.

This proximity-dependent risk pattern reflects fundamental atmospheric dispersion physics: dilution increases exponentially with transport distance, whilst deposition losses reduce airborne inventory progressively during transit. Wylfa's location on Anglesey places it approximately 80–100 km from Ireland—sufficiently close that severe accident plumes can reach Ireland before substantial atmospheric dilution or deposition losses occur. In contrast, Heysham (approximately 180 km), Sizewell B (approximately 400 km), and continental facilities (> 600 km) benefit from extended transport periods permitting multiple e-folding times for atmospheric mixing and wet/dry deposition removal. The May 2024 Wylfa scenario combines three adverse factors: short transport distance, sustained northerly flow maintaining plume coherence, and precipitation enhancement accelerating groundshine-generating deposition. This meteorological pattern—characterised by late spring frontal systems with sustained north-to-south trajectories—represents the specific seasonal threat requiring emergency preparedness focus should Wylfa become operational. The dose assessments employed conservative assumptions throughout (continuous outdoor exposure for 36 hours, no sheltering or protective actions, isotope-specific dose coefficients for adult members of the public), yet existing facilities still yielded sub-threshold doses whilst Wylfa approached intervention levels.

The multi-model verification approach strengthens confidence in these proximity-stratified conclusions. For existing facilities, both models converge on sub-threshold impact, with doses ranging from negligible (Heysham, < 0.01 mSv) to low but measurable (Flamanville, Sizewell, Paluel, 0.5–5 mSv). For Hinkley Point C, both models agree on sub-threshold consequences with factor-of-~6 quantitative divergence (FLEXPART 8.53 mSv vs HYSPLIT 1.38 mSv), demonstrating reasonable inter-model agreement for elevated-consequence scenarios. For Wylfa, the factor-of-~5 disagreement (FLEXPART 20.7 mSv vs HYSPLIT 4.5 mSv over 36 hours) places both predictions in a range where sustained releases could approach Irish intervention levels, with both models identifying this facility as uniquely concerning. The systematic pattern of inter-model variability increasing with consequence magnitude reflects the methodological differences in deposition field representation (near-surface concentration proxy versus explicit deposition schemes) combined with wet deposition parameterisation divergence, exacerbated in near-source scenarios where small-scale meteorological features and surface characteristics exert dominant influence. For emergency preparedness applications, where decisions must be made under uncertainty, the dual-model framework provides credible risk stratification: existing facilities pose low concern (all scenarios well below intervention thresholds), Hinkley warrants monitoring (both models well below 50 mSv), Wylfa requires robust emergency capabilities (36-hour doses suggest potential threshold exceedance under sustained release scenarios). This risk-informed categorisation remains valid despite inter-model quantitative differences, demonstrating that multi-model consensus on relative risk hierarchy provides more value than pursuing spurious numerical precision from single deterministic predictions.

4.3 Atmospheric Drivers of Radiological Consequences

The global sensitivity analysis (Section 3.4) revealed that meteorological conditions, rather than release parameters, dominate consequence severity for events impacting Ireland. Total-order Sobol' indices for release height and duration were consistently below 0.001, indicating negligible contribution to output variance amongst impactful scenarios. In contrast, wind-related variables—particularly kurtosis of west-east wind at 1000 m and median wind speed at 10 m—ranked as the most influential parameters across multiple nuclear power plants and output metrics. The kurtosis metric, measuring the degree of extreme events in wind speed distributions, proved more influential than mean or median wind speed, indicating that infrequent strong-wind events drive highest-consequence transport scenarios rather than typical conditions.

Geopotential height skewness appeared frequently amongst the top three influential variables, particularly for facilities requiring longer transport distances (Flamanville, Paluel, Sizewell). This variable serves as a proxy for atmospheric pressure structure; its skewness quantifies asymmetry in pressure gradient distributions and correlates with frontal passages and synoptic-scale weather systems. The consistent appearance of this parameter suggests that worst-case transport scenarios for Ireland frequently coincide with active frontal systems providing both strong advection and precipitation-driven wet deposition enhancement.

These findings carry important implications for operational emergency response. During the early phase of a nuclear accident, substantial uncertainty typically surrounds source term characteristics including release timing, duration, and effective height. The sensitivity analysis demonstrates that, for events impacting Ireland, consequence severity is governed primarily by meteorological conditions rather than these source term

details. Emergency response priorities should therefore emphasise accurate real-time meteorological forecasting and rapid atmospheric model execution over protracted source term refinement during initial response phases. Meteorological monitoring should prioritise variables identified as influential by the sensitivity analysis, particularly upper-level wind patterns at 1000 m and surface pressure gradients. Notably, for proximal facilities (Wylfa, Heysham), geopotential height appears infrequently or not at all amongst the top three sensitivity drivers, with wind variables predominantly governing consequence severity. In contrast, for more distant sites (Hinkley, Sizewell), geopotential height consistently ranks as the second or third most influential variable, reflecting the greater importance of synoptic-scale pressure patterns in determining whether plumes traverse extended transport distances to reach Ireland.

4.4 Seasonal and Geographical Patterns

The fourteen-year systematic screening revealed distinct seasonal patterns in atmospheric transport probability and intensity (Section 3.1). Spring months, particularly April, consistently exhibited elevated plume intersection frequencies across all nuclear power plants, reflecting the climatology of North Atlantic cyclogenesis and associated easterly or southeasterly flow patterns. Worst-case scenarios concentrated during transitional seasons, with spring (March–May) accounting for seven of eighteen scenarios and autumn (September–October) contributing five scenarios. Late summer months (July–August) consistently ranked as lowest-risk periods, reflecting the dominance of westerly flow and anticyclonic conditions during this season.

Geographical proximity exerted the expected strong influence on maximum deposition values, with Wylfa achieving the highest unit-release deposition ($3.19 \times 10^{-8} \text{ kg m}^{-2}$) due to short transport distance and minimal intervening dilution. However, proximity did not guarantee shortest warning times: the minimum plume arrival scenario (3 hours) occurred for three facilities simultaneously (Heysham, Hinkley Point C, Wylfa) during a particularly favourable synoptic pattern on 25 April 2012, characterised by strong westerly to northwesterly flow. This finding demonstrates that synoptic-scale meteorological conditions can temporarily equalise transport times from facilities at differing distances, with implications for monitoring network design and alert protocols.

Release parameter analysis demonstrated that fourteen of eighteen worst-case scenarios involved extended release durations (48 hours), consistent with severe accident sequences characterised by prolonged containment degradation rather than catastrophic early failure. Release heights clustered at the extremes of the examined range, with elevated releases (50–100 m) dominating maximum deposition scenarios due to reduced near-source dry deposition and enhanced long-range transport capability. These parametric findings align with Level 2 probabilistic safety assessment predictions for contemporary reactor designs, where containment failure modes typically occur many hours after core damage initiation.

4.5 Machine Learning for Rapid Impact Prediction

The XGBoost classification models achieved validation accuracies of 85.4–92.5% for predicting atmospheric impact occurrence based on meteorological conditions and release parameters (Section 3.3). Models for proximal facilities (Wylfa, Heysham) exhibited higher recall (0.76–0.78), correctly identifying most true impact events whilst accepting moderate false-positive rates. Models for distant facilities (Paluel, Flamanville, Sizewell) achieved higher specificity (0.96–0.97), effectively ruling out non-impact scenarios whilst accepting lower sensitivity. This performance gradient reflects the underlying class imbalance: distant facilities impact Ireland less frequently, favouring high-specificity classifiers that minimise false alarms.

Feature importance analysis revealed consistency with the global sensitivity analysis findings, with geopotential height, surface pressure, and wind-related variables ranking as most influential predictors. This convergence of results across fundamentally different methodologies (variance-based sensitivity analysis versus tree-based feature importance) strengthens confidence in the identification of critical atmospheric parameters. The machine learning models provide complementary capability to traditional dispersion modelling: whilst HYSPLIT and FLEXPART require meteorological forecast fields and several hours of computation time, the trained XGBoost models execute in milliseconds and can process ensemble weather forecasts to provide probabilistic impact predictions during the early phase of an event.

Operational deployment of these models could support rapid screening of meteorological forecast ensembles to identify high-probability transport scenarios toward Ireland, enabling pre-positioning of monitoring

resources and alert protocols. The models' demonstrated ability to generalise to unseen 2024 validation data suggests robustness to inter-annual meteorological variability, though periodic retraining with updated meteorological data would be advisable to account for potential climate-driven shifts in atmospheric circulation patterns.

4.6 Methodological Strengths and Limitations

The primary methodological strength of this study lies in the convergence of multiple complementary approaches toward consistent conclusions. The systematic fourteen-year HYSPLIT screening provided statistical robustness through large ensemble size (2.2 million simulations total), substantially exceeding previous Irish assessments in temporal coverage. Independent FLEXPART verification of worst-case scenarios demonstrated multi-model consensus on negligible radiological impact, addressing the fundamental limitation of single-model studies. Machine learning and sensitivity analysis, both leveraging the same simulation ensemble generated for worst-case identification, provided mechanistic understanding of atmospheric drivers whilst maximising the value extracted from the substantial computational investment, enabling prioritisation of monitoring and forecasting resources.

Several limitations warrant acknowledgement. The atmospheric dispersion models employed horizontal resolutions of 0.25 degrees (approximately 20–25 km), adequate for long-range transport but insufficient for resolving sub-grid-scale terrain features or coastal effects that may influence local deposition patterns. Deposition parameterisations employed representative values for aerosol-phase fission products but did not account for particle size distribution evolution during transport or isotope-specific chemical behaviour. The severe accident source terms, whilst based on Level 2 probabilistic safety assessment for late containment failure, necessarily simplified the complex temporal evolution of releases that would occur during actual accident sequences.

The study focused exclusively on atmospheric transport pathways, neglecting potential marine transport following deposition to the Irish Sea or English Channel. For isotopes with long environmental half-lives (cesium-137, plutonium isotopes), marine transport and subsequent incorporation into seafood pathways could provide delayed exposure routes not captured by the 36-hour atmospheric assessment window. However, previous RPII assessments that investigated marine transport pathways from UK nuclear facilities concluded that radiological impacts via this route were negligible [27]. Future work incorporating coupled atmosphere-ocean transport models would nonetheless provide more comprehensive consequence assessment for coastal receptors.

The unit-release screening methodology enabled efficient identification of meteorologically worst-case transport patterns but required subsequent application of realistic source terms for radiological assessment. An alternative approach employing full multi-isotope releases for all 2.2 million simulations would have eliminated this two-stage process but at prohibitive computational cost. The demonstrated consistency between unit-release screening results and full-physics verification simulations validates the adopted methodology for future applications.

4.7 Implications for Emergency Preparedness and Public Communication

The findings of this study have direct implications for Ireland's nuclear emergency preparedness strategies. The demonstration that even worst-case meteorological scenarios produce doses orders of magnitude below intervention thresholds suggests that emergency response priorities should emphasise accurate public communication and minimisation of unnecessary disruption over immediate large-scale protective actions. Historical evidence from Fukushima and Chernobyl demonstrates that public anxiety, economic disruption, and unnecessary evacuation can produce greater societal harm than the radiological consequences themselves for areas receiving low-level contamination [3, 29, 30].

The seasonal patterns identified in this analysis (spring maxima, summer minima for transport probability) could inform resource allocation decisions, with enhanced monitoring readiness and staff availability during higher-risk periods. The machine learning models provide capability for rapid preliminary assessment during the initial phase of an event, before detailed atmospheric dispersion calculations are feasible, enabling earlier public communication and stakeholder engagement.

The identified worst-case scenarios (Table 2) provide specific test cases for emergency response exercises

and decision support system validation. Regular training exercises employing these scenarios would ensure that response personnel are familiar with the range of plausible atmospheric transport patterns and associated timescales for decision-making. The multi-model verification results demonstrate the importance of maintaining multiple independent dispersion modelling capabilities to provide confidence intervals around predictions rather than single deterministic values.

Perhaps most importantly, the quantitative demonstration of minimal radiological impact under worst-case conditions provides an evidence base for public communication regarding nuclear safety. Whilst nuclear accidents at nearby facilities would undoubtedly generate substantial public concern and media attention, the ability to provide quantitative context—comparing predicted doses to natural background radiation, medical procedures, or routine activities—would support informed decision-making and potentially mitigate unnecessary anxiety. The findings should not diminish the importance of robust emergency preparedness but rather inform appropriate calibration of response measures to predicted consequence severity.

5 Conclusions

This study presents the most comprehensive quantitative assessment to date of potential transboundary radiological transport to Ireland from nuclear power plants in the United Kingdom and France. Through systematic screening of 2.2 million HYSPLIT atmospheric dispersion simulations spanning fourteen years (2011–2024), independent verification using FLEXPART, machine learning for rapid impact prediction, and global sensitivity analysis, the research establishes a robust, evidence-based foundation for Ireland’s nuclear emergency preparedness planning.

The central finding provides substantial reassurance regarding existing operational facilities: even under meteorologically worst-case conditions, realistic severe accident releases produce radiological doses to Ireland dramatically below intervention thresholds. Across all existing facilities, 36-hour doses range from negligible (Heysham, <0.01 mSv) through low (Sizewell, Flamanville, Paluel, 0.5–5 mSv) to elevated but sub-threshold (Hinkley, 1–9 mSv). Even when extrapolated to the 7-day assessment period used in international criteria, all existing facilities remain well below the IAEA generic criterion of 100 mSv [20] and Irish intervention levels of 50 mSv for sheltering [11]. This safety margin reflects realistic severe accident source terms, substantial atmospheric dilution during transport, and Ireland’s geographical separation from these facilities.

However, the analysis identifies Wylfa as requiring particular attention. The 36-hour cumulative doses of 4.5–20.7 mSv predicted for worst-case Wylfa scenarios, whilst below thresholds for single-event exposure, suggest that sustained releases coinciding with persistent easterly flow could approach or exceed Irish intervention levels when extrapolated to the 7-day assessment period. This finding warrants continued vigilance regarding any future development at the Wylfa site, given its extreme proximity to Ireland (approximately 80–100 km).

Independent verification using FLEXPART demonstrated robust multi-model consensus on this fundamental conclusion of minimal radiological impact, despite inter-model differences of up to a factor of ~ 10 in absolute dose magnitudes. This verification addresses a critical limitation of single-model assessments and provides confidence that predicted transport patterns represent genuine atmospheric phenomena rather than model-specific artefacts. For emergency preparedness applications requiring decisions under uncertainty, the demonstration of multi-model agreement on dose order-of-magnitude constitutes substantially stronger evidence than reliance on deterministic predictions from individual models.

Global sensitivity analysis revealed that meteorological conditions, rather than release parameters, dominate consequence severity for events impacting Ireland. Wind-related variables—particularly kurtosis of west-east wind at 1000 m and median wind speed at 10 m—ranked as most influential parameters, with release height and duration contributing negligibly to output variance (Sobol’ indices < 0.001). This finding has important operational implications: emergency response priorities should emphasise accurate meteorological forecasting and rapid atmospheric model execution over protracted source term refinement during initial response phases. Meteorological monitoring should prioritise upper-level wind patterns and surface pressure gradients identified as primary drivers of consequence variability.

Machine learning models (XGBoost) achieved validation accuracies of 85.4–92.5% for predicting atmospheric impact occurrence, providing capability for rapid preliminary assessment during the early phase of events before detailed dispersion calculations are feasible. Feature importance analysis demonstrated consistency with sensitivity analysis findings, with geopotential height, surface pressure, and wind variables ranking as most influential predictors. This convergence across fundamentally different methodologies strengthens confidence in the identification of critical atmospheric parameters requiring monitoring prioritisation.

The systematic fourteen-year screening revealed distinct seasonal patterns in atmospheric transport probability, with spring months (particularly April) exhibiting elevated plume intersection frequencies and worst-case scenarios concentrating during transitional seasons. Late summer months (July–August) consistently ranked as lowest-risk periods. Fourteen of eighteen worst-case scenarios involved extended release durations (48 hours), consistent with severe accident sequences characterised by prolonged containment degradation rather than catastrophic early failure. These temporal and parametric patterns provide actionable intelligence for emergency preparedness resource allocation and exercise planning.

Several recommendations emerge from this research for enhancing Ireland’s nuclear emergency preparedness capabilities. First, the demonstrated importance of meteorological conditions in governing consequence severity emphasises the need for sustained investment in high-quality meteorological forecasting and ensemble prediction systems. Second, the multi-model verification results demonstrate the value of maintaining

multiple independent atmospheric dispersion modelling capabilities to provide confidence intervals around predictions rather than single deterministic values. Third, the machine learning models developed in this study should be integrated into operational decision support systems to enable rapid preliminary impact assessment during the initial phase of events. Fourth, the identified worst-case scenarios provide specific test cases for regular emergency response exercises, ensuring that response personnel are familiar with the range of plausible atmospheric transport patterns and associated decision-making timescales.

Fifth, and perhaps most importantly, the quantitative demonstration of minimal radiological impact under worst-case conditions provides an evidence base for calibrated public communication. Whilst nuclear accidents at nearby facilities would undoubtedly generate substantial public concern, the ability to provide quantitative context—comparing predicted doses to natural background radiation and routine activities—would support informed decision-making and potentially mitigate unnecessary anxiety and disruption. Emergency response protocols should be calibrated to predicted consequence severity rather than worst-case assumptions decoupled from realistic atmospheric transport and source term physics.

Future research directions could usefully address several limitations identified in this study. Coupled atmosphere-ocean transport models would provide more comprehensive consequence assessment for coastal receptors, capturing marine transport pathways and seafood incorporation for long-lived isotopes. Higher-resolution nested dispersion modelling would better resolve sub-grid-scale terrain features and coastal effects influencing local deposition patterns. Explicit treatment of particle size distribution evolution and isotope-specific chemical behaviour would refine deposition predictions. Integration of the atmospheric transport findings with Level 3 probabilistic safety assessment could provide fully probabilistic consequence estimates incorporating both accident frequency and meteorological variability.

Notwithstanding these potential refinements, the current study establishes a comprehensive, quantitative foundation for Ireland's nuclear emergency preparedness. The convergence of findings across multiple methodologies—large-ensemble screening, multi-model verification, machine learning, and sensitivity analysis—provides robust evidence that Ireland's geographical separation from major nuclear facilities, combined with modern reactor safety systems and realistic severe accident physics, results in minimal radiological consequences even under meteorologically worst-case conditions. This evidence base should inform appropriate calibration of emergency response measures, resource allocation, and public communication strategies, ensuring that Ireland maintains effective preparedness whilst avoiding unnecessary disruption and anxiety based on overly conservative assumptions disconnected from realistic consequence assessment.

References

- [1] AREVA NP and EDF SA. PCSR – sub-chapter 16.2 – severe accident analysis (RRC-B). Technical Report UKEPR-0002-162 Issue 05, EDF Energy / AREVA NP, November 2012. Pre-Construction Safety Report (PCSR) submitted for UK EPR Generic Design Assessment. The 4900 MWth core inventory assumption is detailed in Section 3.2.1 (page 239/295). URL: <https://www.yumpu.com/en/document/view/49726648/162-severe-accident-analysis-rrc-b-edf-hinkley-point>.
- [2] L. Bakels, S. Henne, C. Hüglin, D. Brunner, L. Emmenegger, and I. Pisso. FLEXPART version 11: improved accuracy, efficiency, and flexibility. *Geoscientific Model Development*, 17:7595–7627, 2024. [doi:10.5194/gmd-17-7595-2024](https://doi.org/10.5194/gmd-17-7595-2024).
- [3] E. J. Bromet, J. M. Havenga, and L. T. Guey. A 25 year retrospective review of the psychological consequences of the Chernobyl accident. *Clinical Oncology*, 23(4):297–305, 2011. [doi:10.1016/j.clon.2011.01.501](https://doi.org/10.1016/j.clon.2011.01.501).
- [4] T. Chai, R. Draxler, and A. Stein. Source term estimation using air concentration measurements and a Lagrangian dispersion model: Experiments with pseudo and real cesium-137 observations from the Fukushima nuclear accident. *Atmospheric Environment*, 106:241–251, 2015. [doi:10.1016/j.atmosenv.2015.01.070](https://doi.org/10.1016/j.atmosenv.2015.01.070).
- [5] E. Cheynet, J. B. Jakobsen, and J. Reuder. Tall wind profile validation of ERA5, NORA3, and NEWA datasets using lidar observations. *Wind Energy Science*, 10:733–754, 2025. [doi:10.5194/wes-10-733-2025](https://doi.org/10.5194/wes-10-733-2025).
- [6] O. Connan, K. Smith, C. Organo, L. Solier, D. Maro, and D. Hébert. Comparison of RIMPUFF, HYSPLIT, ADMS atmospheric dispersion model outputs, using emergency response procedures, with ^{85}Kr measurements made in the vicinity of nuclear reprocessing plant. *Journal of Environmental Radioactivity*, 124:266–277, 2013. [doi:10.1016/j.jenvrad.2013.06.004](https://doi.org/10.1016/j.jenvrad.2013.06.004).
- [7] Thierry Crestaux, Olivier Le Maître, and Jean-Marc Martinez. Polynomial chaos expansion for sensitivity analysis. *Reliability Engineering & System Safety*, 94(7):1161–1172, 2009. Special Issue on Sensitivity Analysis. [doi:10.1016/j.ress.2008.10.008](https://doi.org/10.1016/j.ress.2008.10.008).
- [8] Roland R. Draxler and G. D. Hess. An overview of the hysplit_4 modelling system for trajectories, dispersion, and deposition. *Australian Meteorological Magazine*, 47(4):295–308, 1998. URL: <https://www.arl.noaa.gov/documents/reports/MetMag.pdf>.
- [9] K. Eckerman, J. Harrison, H-G. Menzel, and C. H. Clement. Compendium of dose coefficients based on ICRP publication 60. *Annals of the ICRP*, 41(Suppl.), 2012. ICRP Publication 119. Authors on behalf of ICRP. URL: <https://journals.sagepub.com/doi/pdf/10.1016/j.icrp.2013.05.003>, [doi:10.1016/j.icrp.2013.05.003](https://doi.org/10.1016/j.icrp.2013.05.003).
- [10] Environmental Protection Agency. Potential radiological impact on Ireland of postulated accidents at the Sellafield nuclear fuel reprocessing plant. Technical report, Environmental Protection Agency, Dublin, Ireland, 2016. EPA Report RPII-15/01. URL: https://www.epa.ie/publications/compliance--enforcement/radiation/Potential_radiological_impact_Ireland.pdf.
- [11] Environmental Protection Agency. National plan for nuclear and radiological emergency exposures. Technical report, Environmental Protection Agency, Ireland, 2019. URL: <https://www.epa.ie/publications/monitoring--assessment/radiation/National-Plan-for-Nuclear-and-Radiological-Emergency-Exposures.pdf>.
- [12] S. Galmarini, R. Bianconi, W. Klug, T. Mikkelsen, R. Addis, S. Andronopoulos, P. Astrup, A. Baklanov, J. Bartniki, J. C. Bartzis, R. Bellasio, F. Bompay, R. Buckley, M. Bouzoum, H. Champion, R. D'Amours, E. Davakis, H. Eleveld, G. T. Geertsema, H. Glaab, M. Kollax, M. Ilvonen, A. Manning, U. Pechinger, C. Persson, E. Polreich, S. Potemski, M. Prodanova, J. Saltbones, H. Slaper, M. A.

Sofiev, D. Syrakov, J. H. Sørensen, L. Van der Auwera, I. Valkama, and R. Zelazny. Ensemble dispersion forecasting—Part I: concept, approach and indicators. *Atmospheric Environment*, 38(28):4607–4617, 2004. URL: <https://www.sciencedirect.com/science/article/pii/S1352231004004959>, doi:10.1016/j.atmosenv.2004.05.030.

[13] S. Girard, I. Korsakissok, and V. Mallet. Emulation and Sobol' sensitivity analysis of an atmospheric dispersion model applied to the Fukushima nuclear accident. *Journal of Geophysical Research: Atmospheres*, 121:3484–3496, 2016. doi:10.1002/2015JD023993.

[14] J. Guo, J. Zhang, K. Yang, H. Liao, S. Zhang, K. Huang, Y. Lv, J. Shao, T. Yu, B. Tong, J. Li, T. Su, S. H. L. Yim, A. Stoffelen, P. Zhai, and X. Xu. Investigation of near-global daytime boundary layer height using high-resolution radiosondes: first results and comparison with ERA5, MERRA-2, JRA-55, and NCEP-2 reanalyses. *Atmospheric Chemistry and Physics*, 21(22):17079–17097, 2021. URL: <https://acp.copernicus.org/articles/21/17079/2021/>, doi:10.5194/acp-21-17079-2021.

[15] M. A. Hernández-Ceballos, M. Sangiorgi, B. García-Puerta, M. Montero, and C. Trueba. Dispersion and ground deposition of radioactive material according to airflow patterns for enhancing the preparedness to N/R emergencies. *Journal of Environmental Radioactivity*, 216:106178, May 2020. doi:10.1016/j.jenvrad.2020.106178.

[16] H. Hersbach, B. Bell, P. Berrisford, S. Hirahara, A. Horányi, J. Muñoz-Sabater, J. Nicolas, C. Peubey, R. Radu, D. Schepers, A. Simmons, C. Soci, S. Abdalla, X. Abellán, G. Balsamo, P. Bechtold, G. Biavati, J. Bidlot, M. Bonavita, G. De Chiara, P. Dahlgren, D. Dee, M. Diamantakis, R. Dragani, J. Flemming, R. Forbes, M. Fuentes, A. Geer, L. Haimberger, S. Healy, R. J. Hogan, E. Hólm, M. Janisková, S. Keeley, P. Laloyaux, P. Lopez, C. Lupu, G. Radnoti, P. de Rosnay, I. Rozum, F. Vamborg, S. Villaume, and J.-N. Thépaut. The ERA5 global reanalysis. *Quarterly Journal of the Royal Meteorological Society*, 146:1999–2049, 2020. doi:10.1002/qj.3803.

[17] ICRP. The 2007 recommendations of the International Commission on Radiological Protection. *ICRP Publication 103, Annals of the ICRP*, 37(2-4), 2007. URL: https://journals.sagepub.com/doi/pdf/10.1177/ANIB_37_2-4, doi:10.1016/j.icrp.2007.10.003.

[18] ICRP. ICRP publication 158: Dose coefficients for intakes of radionuclides by members of the public: Part 1. *Annals of the ICRP*, 53(4-5):1–355, 2024. Approved by the Commission in March 2023. URL: <https://pubmed.ncbi.nlm.nih.gov/41202001/>, doi:10.1177/01466453241248229.

[19] International Atomic Energy Agency. *Preparedness and response for a nuclear or radiological emergency*. Number GSR Part 7. IAEA, Vienna, Austria, 2015. URL: <https://www.iaea.org/publications/10905/preparedness-and-response-for-a-nuclear-or-radiological-emergency>.

[20] International Atomic Energy Agency. Preparedness and response for a nuclear or radiological emergency: General safety requirements. Technical Report GSR Part 7, Vienna, November 2015. Jointly sponsored by FAO, IAEA, ICAO, ILO, IMO, INTERPOL, OECD/NEA, PAHO, CTBTO, UNEP, OCHA, WHO, WMO. URL: https://www-pub.iaea.org/MTCD/Publications/PDF/P_1708_web.pdf.

[21] P. D. Ivatt and M. J. Evans. Improving the prediction of an atmospheric chemistry transport model using gradient-boosted regression trees. *Atmospheric Chemistry and Physics*, 20:8063–8082, 2020. doi:10.5194/acp-20-8063-2020.

[22] Cillian Joy. *Modelling of accidental radioactive releases for Ireland*. PhD thesis, School of Physics, College of Science, Centre for Climate & Air Pollution Studies, National University of Ireland Galway, January 2020. Supervisor: Professor Colin O'Dowd; Co-supervisor: Dr Damien Martin. URL: <https://researchrepository.universityofgalway.ie/bitstreams/02095373-61ad-4bcc-9208-da4587b43a3d/download>.

[23] G. Katata, M. Ota, H. Terada, M. Chino, and H. Nagai. Detailed source term estimation of the atmospheric release for the Fukushima Daiichi Nuclear Power Station accident by coupling simulations of an atmospheric dispersion model with an improved deposition scheme and oceanic dispersion model. *Atmospheric Chemistry and Physics*, 15:1029–1070, 2015. doi:10.5194/acp-15-1029-2015.

[24] S. J. Leadbetter, S. Andronopoulos, P. Bedwell, K. Chevalier-Jabet, G. Geertsema, F. Gering, T. Hamberger, A. R. Jones, H. Klein, I. Korsakissok, A. Mathieu, T. Pázmándi, R. Périllat, Cs. Rudas, A. Sogachev, P. Szántó, J. M. Tomas, C. Twenhoefel, H. de Vries, and J. Wellings. Ranking uncertainties in atmospheric dispersion modelling following the accidental release of radioactive material. *Radioprotection*, 55:S51–S55, 2020. [doi:10.1051/radiopro/2020012](https://doi.org/10.1051/radiopro/2020012).

[25] S. J. Leadbetter, A. R. Jones, and M. C. Hort. Assessing the value meteorological ensembles add to dispersion modelling using hypothetical releases. *Atmospheric Chemistry and Physics*, 22(1):577–596, 2022. URL: <https://acp.copernicus.org/articles/22/577/2022/>, doi:10.5194/acp-22-577-2022.

[26] B. Liu, X. Tan, Y. Jin, et al. Application of RR-XGBoost combined model in data calibration of micro air quality detector. *Scientific Reports*, 11:15662, 2021. [doi:10.1038/s41598-021-95027-1](https://doi.org/10.1038/s41598-021-95027-1).

[27] C. McMahon, K. Kelleher, P. McGinnity, C. Organo, K. Smith, L. Curran, and T. Ryan. Proposed nuclear power plants in the UK – potential radiological implications for Ireland. Technical Report RPII 13/01, Radiological Protection Institute of Ireland (RPII), Dublin, May 2013. URL: <https://inis.iaea.org/records/v87z0-s3r24>.

[28] B. E. Moroz, C. S. Lim, M. A. Caffrey, A. F. Turner, S. K. Rope, D. Arnold, and R. R. Draxler. Predictions of dispersion and deposition of fallout from nuclear testing using the NOAA-HYSPLIT meteorological model. *Health Physics*, 99(2):252–269, 2010. [doi:10.1097/HP.0b013e3181b43697](https://doi.org/10.1097/HP.0b013e3181b43697).

[29] Michio Murakami, Kyoko Ono, Masaharu Tsubokura, Shuhei Nomura, Tomoyoshi Oikawa, Toshihiro Oka, Masahiro Kami, and Taikan Oki. Was the risk from nursing-home evacuation after the Fukushima accident higher than the radiation risk? *PLOS ONE*, 10(9):e0137906, 2015. [doi:10.1371/journal.pone.0137906](https://doi.org/10.1371/journal.pone.0137906).

[30] Shuhei Nomura, Stuart Gilmour, Masaharu Tsubokura, Daisuke Yoneoka, Akihiko Sugimoto, Tomoyoshi Oikawa, Masahiro Kami, and Kenji Shibuya. Mortality risk amongst nursing home residents evacuated after the Fukushima nuclear accident: a retrospective cohort study. *PLOS ONE*, 8(3):e60192, 2013. [doi:10.1371/journal.pone.0060192](https://doi.org/10.1371/journal.pone.0060192).

[31] N. Petoussi-Henss, W. E. Bolch, K. F. Eckerman, A. Endo, N. Hertel, J. Hunt, M. Pelliccioni, H. Schlattl, and M. Zankl. ICRP publication 144: Dose coefficients for external exposures to environmental sources. *Annals of the ICRP*, 49(2):11–145, 2020. [doi:10.1177/0146645320906277](https://doi.org/10.1177/0146645320906277).

[32] I. Pisso, E. Sollum, H. Grythe, N. I. Kristiansen, M. Cassiani, S. Eckhardt, D. Arnold, D. Morton, R. L. Thompson, C. D. Groot Zwaaftink, N. Evangelou, H. Sodemann, L. Haimberger, S. Henne, D. Brunner, J. F. Burkhardt, A. Fouilloux, J. Brioude, A. Philipp, P. Seibert, and A. Stohl. FLEXPART version 10.4. *Geoscientific Model Development*, 12:4955–4997, 2019. [doi:10.5194/gmd-12-4955-2019](https://doi.org/10.5194/gmd-12-4955-2019).

[33] M. M. Rajabi, B. Ataie-Ashtiani, and C. T. Simmons. Polynomial chaos expansions for uncertainty propagation and moment independent sensitivity analysis of seawater intrusion simulations. *Journal of Hydrology*, 520:101–122, 2015. [doi:10.1016/j.jhydrol.2014.11.020](https://doi.org/10.1016/j.jhydrol.2014.11.020).

[34] E. Ryan, O. Wild, A. Voulgarakis, and L. Lee. Fast sensitivity analysis methods for computationally expensive models with multi-dimensional output. *Geoscientific Model Development*, 11:3131–3146, 2018. [doi:10.5194/gmd-11-3131-2018](https://doi.org/10.5194/gmd-11-3131-2018).

[35] Yousuke Sato, Tsuyoshi Thomas Sekiyama, Sheng Fang, Mizuo Kajino, Arnaud Quérel, Denis Quélo, Hiroaki Kondo, Hiroaki Terada, Masanao Kadokawa, Masayuki Takigawa, Yu Morino, Junya Uchida, Daisuke Goto, and Hiromi Yamazawa. A model intercomparison of atmospheric ^{137}Cs concentrations from the Fukushima Daiichi Nuclear Power Plant accident, phase III: Simulation with an identical source term and meteorological field at 1-km resolution. *Atmospheric Environment: X*, 7:100086, 2020. URL: <https://www.sciencedirect.com/science/article/pii/S2590162120300253>, doi:10.1016/j.aaea.2020.100086.

[36] O. Saunier, A. Mathieu, D. Didier, M. Tombette, D. Quélo, V. Winiarek, and M. Bocquet. An inverse modeling method to assess the source term of the Fukushima Daiichi nuclear power plant accident using gamma dose rate observations. *Atmospheric Chemistry and Physics*, 13:11403–11421, 2013. [doi:10.5194/acp-13-11403-2013](https://doi.org/10.5194/acp-13-11403-2013).

[37] O. Skrynyk, V. Voloshchuk, I. Budak, and S. Bubin. Regional HYSPLIT simulation of atmospheric transport and deposition of the Chernobyl ^{137}Cs releases. *Atmospheric Pollution Research*, 10(6):1953–1963, November 2019. [doi:10.1016/j.apr.2019.09.001](https://doi.org/10.1016/j.apr.2019.09.001).

[38] L. Soffer, S. B. Burson, C. M. Ferrell, R. Y. Lee, and J. N. Ridgely. Accident source terms for light-water nuclear power plants. Technical Report NUREG-1465, U.S. Nuclear Regulatory Commission, Washington, DC, February 1995. Defines alternative radiological source terms for design basis accidents and severe accidents in PWR and BWR reactors, including release timing and magnitude. NRC ADAMS Accession No. ML041040063. URL: <https://www.nrc.gov/reading-rm/doc-collections/nuregs/staff/sr1465/index>.

[39] Bruno Sportisse. A review of parameterizations for modelling dry deposition and scavenging of radionuclides. *Atmospheric Environment*, 41(13):2683–2698, 2007. [doi:10.1016/j.atmosenv.2006.11.057](https://doi.org/10.1016/j.atmosenv.2006.11.057).

[40] A. F. Stein, R. R. Draxler, G. D. Rolph, B. J. B. Stunder, M. D. Cohen, and F. Ngan. NOAA’s HYSPLIT atmospheric transport and dispersion modeling system. *Bulletin of the American Meteorological Society*, 96(12):2059–2077, 2015. [doi:10.1175/BAMS-D-14-00110.1](https://doi.org/10.1175/BAMS-D-14-00110.1).

[41] A. Stohl, C. Forster, A. Frank, P. Seibert, and G. Wotawa. Technical note: The Lagrangian particle dispersion model FLEXPART version 6.2. *Atmospheric Chemistry and Physics*, 5:2461–2474, 2005. [doi:10.5194/acp-5-2461-2005](https://doi.org/10.5194/acp-5-2461-2005).

[42] A. Stohl, M. Hittenberger, and G. Wotawa. Validation of the Lagrangian particle dispersion model FLEXPART against large-scale tracer experiment data. *Atmospheric Environment*, 32(24):4245–4264, 1998. [doi:10.1016/S1352-2310\(98\)00184-8](https://doi.org/10.1016/S1352-2310(98)00184-8).

[43] Masanori Takeyasu and Shuichi Sumiya. Estimation of dry deposition velocities of radionuclides released by the accident at the Fukushima Dai-ichi Nuclear Power Plant. *Progress in Nuclear Science and Technology*, 4:64–67, April 2014. [doi:10.15669/pnst.4.64](https://doi.org/10.15669/pnst.4.64).

[44] Sevtap Tirink. Machine learning-based forecasting of air quality index under long-term environmental patterns: A comparative approach with XGBoost, LightGBM, and SVM. *PLOS ONE*, 20(10):e0334252, October 2025. [doi:10.1371/journal.pone.0334252](https://doi.org/10.1371/journal.pone.0334252).

[45] Bärbel Vogel, C. Michael Volk, Johannes Wintel, Valentin Lauther, Jan Clemens, Jens-Uwe Grooß, Gebhard Günther, Lars Hoffmann, Johannes C. Laube, Rolf Müller, Felix Ploeger, and Fred Stroh. Evaluation of vertical transport in ERA5 and ERA-Interim reanalysis using high-altitude aircraft measurements in the Asian summer monsoon 2017. *Atmospheric Chemistry and Physics*, 24(1):317–343, January 2024. [doi:10.5194/acp-24-317-2024](https://doi.org/10.5194/acp-24-317-2024).

[46] H. M. Wainwright, S. Finsterle, Y. Jung, Q. Zhou, and J. T. Birkholzer. Making sense of global sensitivity analyses. *Computers & Geosciences*, 65:84–94, 2014. [doi:10.1016/j.cageo.2013.06.006](https://doi.org/10.1016/j.cageo.2013.06.006).

[47] Jeffrey Wang, Daniel Clayton, and Shaheen Azim Dewji. Comparison of atmospheric radionuclide dispersion models for a risk-informed consequence-driven advanced reactor licensing framework. *Journal of Environmental Radioactivity*, 273:107379, March 2024. URL: <https://www.sciencedirect.com/science/article/abs/pii/S0265931X24000110>, [doi:10.1016/j.jenvrad.2024.107379](https://doi.org/10.1016/j.jenvrad.2024.107379).

[48] Steve Warner, Nathan Platt, and James F. Heagy. Comparisons of transport and dispersion model predictions of the European Tracer EXperiment: Area- and population-based user-oriented measures of effectiveness. *Atmospheric Environment*, 39(25):4425–4437, 2005. URL: <https://www.sciencedirect.com/science/article/abs/pii/S135223100500364X>, [doi:10.1016/j.atmosenv.2005.05.002](https://doi.org/10.1016/j.atmosenv.2005.05.002).

Appendix: Complete Dose Assessment Results

Table 9 presents comprehensive dose assessment results for all eighteen worst-case scenarios across six nuclear facilities. Section 3.2 provided detailed spatial analysis of the Heysham maximum deposition scenario as a representative case study, demonstrating model verification methodology and spatial dose distribution patterns.

Table 9: Combined Dose Assessment for Whole of Ireland: All Worst-Case Scenarios

Scenario	Gamma Rate (mSv/h)		Inhalation (mSv)		Total Dose (mSv)	
	FP	HS	FP	HS	FP	HS
Flamanville Max Concentration	0.0172	0.00305	0.00137	0.00249	0.622	0.112
Flamanville Max Deposition	0.128	0.0402	0.00216	0.00623	4.62	1.45
Flamanville Min Plume Arrival	0.000574	0.00126	6.19e-06	1.04e-06	0.0207	0.0453
Heysham Max Concentration	5.51e-06	6.07e-06	2.68e-06	3.26e-06	0.000201	0.000222
Heysham Max Deposition	1.35e-05	0.000186	4.25e-06	2.18e-05	0.000489	0.00671
Heysham Min Plume Arrival	1.25e-06	3.52e-05	4.2e-07	1.3e-07	4.52e-05	0.00127
Hinkley Max Concentration	0.053	0.032	0.00538	0.0249	1.91	1.18
Hinkley Max Deposition	0.237	0.0383	0.00264	0.00233	8.53	1.38
Hinkley Min Plume Arrival	0.00931	0.00768	0.000184	0.000101	0.335	0.277
Paluel Max Concentration	0.0261	0.00311	0.00172	0.00193	0.939	0.113
Paluel Max Deposition	0.0562	0.0132	0.000971	0.00156	2.02	0.474
Paluel Min Plume Arrival	0.0806	0.0101	0.0017	6.2e-05	2.9	0.363
Sizewell Max Concentration	0.00318	0.00416	0.000171	3.51e-06	0.115	0.15
Sizewell Max Deposition	0.0399	0.017	0.000499	0.00146	1.44	0.612
Sizewell Min Plume Arrival	0.0285	0.0151	0.000315	3.01e-05	1.03	0.545
Wylfa Max Concentration	0.516	0.0467	0.0116	0.0389	18.6	1.72
Wylfa Max Deposition	0.574	0.123	0.00963	0.0542	20.7	4.48
Wylfa Min Plume Arrival	0.198	0.0425	0.00414	0.00321	7.12	1.53

Results employ isotope-specific deposition physics with element-based wet scavenging coefficients (Cs/I: $1.0 \times 10^{-4} \text{ s}^{-1}$, Pu/Am/Cm: $2.0 \times 10^{-5} \text{ s}^{-1}$) and dry deposition velocities (Cs/I: $0.0015\text{--}0.002 \text{ m s}^{-1}$, Pu: 0.005 m s^{-1}). All doses represent 36-hour cumulative exposure for the whole of Ireland, calculated using isotope-specific dose coefficients for adult members of the public. Both FLEXPART and HYSPLIT employed identical element-specific parameters to ensure consistent physics between models.